Novel Cosmology

by the Energy Circulation Theory

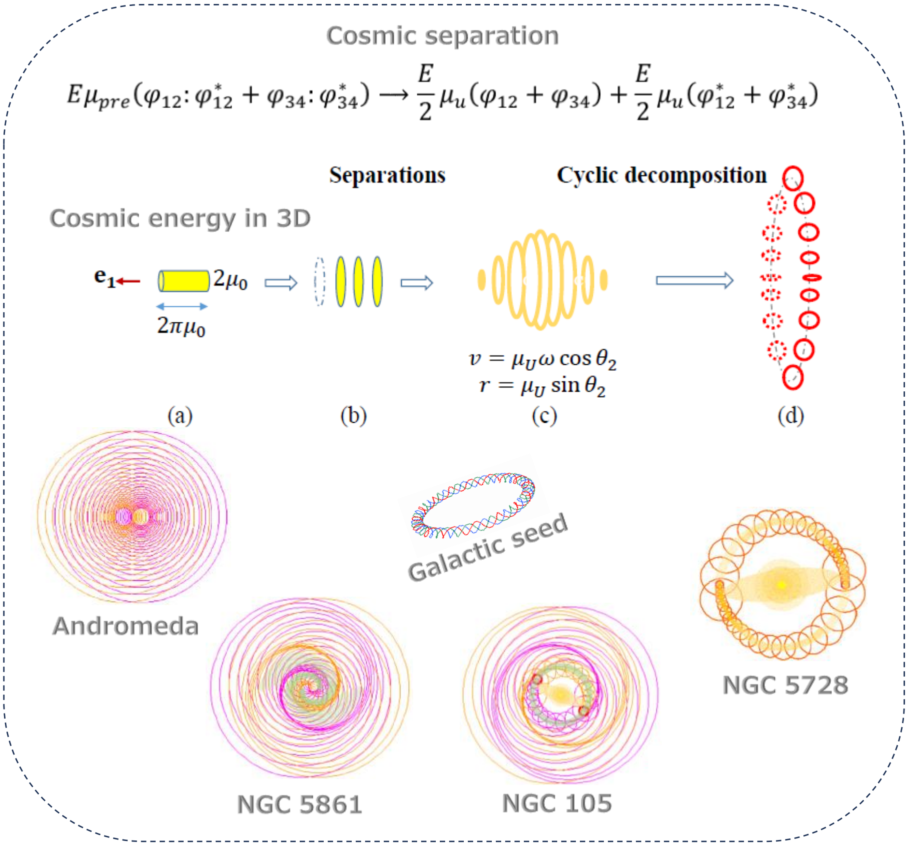

Ver. 2024.05

Shigeto Nagao

Novel cosmology by the energy circulation theory

Table of contents:

Chapter 1: Introduction

1.1. Prologue

In the standard physics, there are too many serious unsolved problems such as dark energy, dark matter, gamma-ray bursts, formation of various shapes of galaxies and so on. Nevertheless, so called the modern physics including the theory of relativity, the quantum mechanics, and the standard particle physics are regarded as absolutely correct with leaving the open questions just as unknown.

If we carefully see the establishments of such modern physics, they were not developed fully logically but were including logical leaps or contradictions. Subsequent physicists swallowed them without verification. Now they are treated as an absolute truth without proofing. Why such a situation has come out? It may have a similarity to the case of the geocentric theory and the heliocentric theory. Before the gravitational force was discovered, various possibilities to explain the complex movements of planets should have been thought to have a chance. Even if some factor or force to cause such motions of planets under the geocentric vision was proposed, it might have been accepted. However, it would be denied after the gravitational force was discovered.

We discovered and published in a paper in 2018 that there works a force between energies based on their movements, that is, momentums. This force was named as the fundamental force. It is in contrast to the gravitational force, which acts based on the amount of energy. Anti-parallel movements of energies form a circular motion due to the centripetal force by the fundamental force. We have investigated a completely new physical system based on the two premises including the fundamental force, and we call it as the "energy circulation theory". Like a miracle, the new theory has been solving the open questions of the existing physics one after another. It has been revealed that all of the electric, magnetic, and nuclear (strong and weak) forces are a presentation of the fundamental force.

Without knowing the fundamental force, they expected the presence of a supermassive black hole at the center of a galaxy in order to explain the galactic rotation in the standard cosmology. Furthermore, to explain the same rotating velocity at any radial distances, they introduced the presence of dark matter in the halo region. However, the galactic rotation and its velocity can be naturally derived once we take the fundamental force. Either such a black hole or dark matter does not exist in fact.

In this book, let us see how has the cosmos developed to the current figures based on the energy circulation theory (ECT). Before this book, the following PDF books on the ECT were released in our website. Please read them if you need supplementary information.

- Discovery of the Energy Circulation Theory
  http://www3.plala.or.jp/MiTiempo/Junshin-E.pdf
- Modern physics full of mistakes
  http://www3.plala.or.jp/MiTiempo/ModernPhysics.pdf
- Novel electromagnetism by the energy circulation theory
  http://www3.plala.or.jp/MiTiempo/NovelEM-E.pdf

In the third book above, we precisely explained the ECT. Since we will focus on the cosmic evolution in this book, please refer to it for further details on the ECT.

1.2. Fundamentals of the energy circulation theory

The energy circulation theory is to develop the essences of the universe logically from scratch. At first, the "**energy**" is defined as anything that exists in the universe. Other physical properties are defined secondarily from energy distribution, motion, and interactions. In the existing physics on the contrary, energy is defined secondarily from mass, acceleration, charge, electric potential, etc.

✧ Starting points of the energy circulation theory: two premises

The energy circulation theory starts from the following two promises.

(1) Energy can be expressed by an intrinsic energy and its velocity, shown by the below formula.

$$E = M_1 {V_1}^2 = M_2 {V_2}^2 = mc^2 \qquad (1)$$

(2) Between energies, the force shown by the below formula works based on their momentums.

$$F = K_f \frac{{}_{\mathrm{r}}\mathbf{p}_1 \cdot {}_{\mathrm{r}}\mathbf{p}_2}{d^2} = K_f \frac{p_1 p_2}{d^2} \cos\theta_p \sin\theta_1 \sin\theta_2 \qquad (2)$$

K_f : Fundamental force constant

Fig. 1. Momentum components to the distance

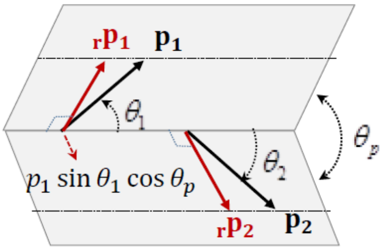

(In addition, gravitational force acts on the amount of energy.)

These two premises are assumptions and correspond to axioms in mathematics. We named the development from these two premises as the "**energy circulation theory ECT**".

✧ Intrinsic energy

There are many ways to select the **intrinsic energy** in (1) depending on the direction to take, etc., but in all combinations, the product of the magnitude of the intrinsic energy and the square of its velocity gives the same energy. The motion in a direction orthogonal to the direction of interest is incorporated in the intrinsic energy. An intrinsic energy has the property of mass, but we define such intrinsic energies that move at the light speed as the "**mass**" in the narrow sense.

✧ Fundamental force

We named the force of (2) as the "**fundamental force**". The **charge** exerting the force is a vector, and the formula includes three angular factors in addition to the distance. We define the "**momentum**" as the product of the intrinsic energy and its velocity by $\mathbf{p} = M\mathbf{V}$. The momentum alters depending on how the intrinsic energy is taken, but if an intrinsic energy of a common velocity is taken, its magnitude is proportional to the amount of the intrinsic energy. As shown in Fig. 1, ${}_{\mathbf{r}}\mathbf{p}$ is the orthogonal component of a momentum to the distance direction in the plane of the momentum and the distance direction, and its amount is given by ${}_{r}p = p\sin\theta$. The magnitude of the fundamental force is the inner product of these components of the two momentums, and the direction is the distance direction. A plus force is repulsive, and a minus force is attractive. Anti-parallel energy movements circulate by attraction of the fundamental force, and form an **energy circulation**. The momentum and the fundamental force constant K_f change depending on how the intrinsic energy is taken, but the force is the same. Unless otherwise mentioned, K_f shall be the fundamental force constant for the intrinsic energies that move at the light speed c (the light speed shall be discussed later).

✧ Novel physics from the energy circulation theory

The energy circulation theory ECT requires an essential restructuring of the existing physics. In 2018, the first article on the ECT was published in Reports in Advances of Physical Sciences. After that, important consequences from the ECT were successively reported, and by now a total of seven papers listed below have been published in the same journal.

[1] Energy circulation theory

It is the first article claiming the ECT with the title of "Energy circulation theory to provide a cosmic evolution, electric charge, light and electromagnetism". Based on the ECT, it reported the cosmic evolution, the origin of the electric charge, the mechanism of light emission and the light speed, summary of the electromagnetism, etc. The light is a wave in hidden-space dimensions.

https://doi.org/10.1142/S242494241850007X

[2] Structures and interactions of quantum particles

For each of major known particles (leptons, mesons, baryons), the composition of energy circulations, energy (mass), spin and decay reactions were shown.

https://doi.org/10.1142/S2424942419500014

[3] Galactic evolution (without dark matter)

Here were reported the cosmic evolution including how galaxies were formed. It is regulated by the fundamental force working on momentums. There neither exists the black hole at the center nor dark matter in the halo, which were assumed in order to explain the galactic rotation and its velocity in the existing physics.

https://doi.org/10.1142/S2424942420500048

[4] Quantum mechanics

Here was explained that the existing quantum mechanics includes some contradictions and essential mistakes. A novel wave equation for particles by the ECT was reported. The wave function for a particle shows its energy distribution in the real space.

https://doi.org/10.1142/S2424942421500018

[5] Gamma-ray bursts

The gamma-ray burst is the phenomenon that gamma-rays are released when a galactic seed separates to two ones, where gravitational waves (waves in space-space dimensions) are also released. The details of the galactic seed separation, and the changes in force and potential energy between the two galactic seeds were shown with mathematical formulas.

https://doi.org/10.1142/S2424942421500055

[6] Formation of various shapes of galaxies

There are many types of galaxies, including ellipse, ring, disc, spiral, and barred spiral ones. Here the formation of each type of them was shown by simulation. In the existing physics, formations of any types remain as mystery.

https://doi.org/10.1142/S2424942422500049

[7] Novel electromagnetism

Based on the ECT, the electric charge, electric current, and magnetic charge were redefined, and the electromagnetism was reconstructed. The magnetic charge density, which corresponds to the magnetic field, around an electric current was quantitively derived.

https://doi.org/10.1142/S2424942423500081

From the Chapter 3, we will refer and explain the key aspects from the above articles [1], [3], [5] and [6] as a novel cosmology. Before that, let us briefly see problems of the existing physics.

Chapter 2: Contradictions and mistakes of modern physics

2.1. Light speed invariance

As a general property of waves, the propagation velocity does not change as the source moves relative to the medium. However, if the observer moves, the propagation velocity by the observer's frame varies by its speed to the medium. Therefore, if the earth moves toward the medium, the light speed should vary depending on the direction to measure. This is called as the **anisotropy** of the light speed.

✧ Michelson-Morley experiment

Michelson and Morley reported experiments on the anisotropy in 1881 and 1887. The light from the source was divided by a half-mirror into a beam reflected to the vertical direction and a transmitted straight beam. Both beams were reflected at the same distance, returned to the half-mirror, and were led to the observation device. If the apparatus is moving relative to the medium, there will be a difference in the propagation velocity between the vertical and horizontal beams. The combined beam passes through two slits apart with a very small distance, propagates radially from each slit, and forms interference fringes on the screen. They thought that when the whole apparatus was rotated, the speed of motion of the light path relative to the medium would change, and the spacing and position of the interference fringes would change. However, they did not detect a notable change in the spacing or position of fringes. After that, many people conducted the similar experiments, but no change was seen. It was then concluded that the light speed is constant regardless of the observer's motion, and further concluded that the light has no medium. This is the famous law of the **light speed invariance** in the standard physics.

✧ Mis-leading from the light speed invariance

This interpretation then evoked the **Lorentz transformation**, which is the essence of the **special relativity**, and the idea that the **space expansion is accelerating**. However, the detection principle of the anisotropy was not fully described even in the Michelson's papers, but they only mentioned to expect a change in fringe positions. Later physicists did not verify the detection principle, either. Since before reported the ECT, we have been claiming time to time that the Michelson-Morley-like experiments cannot detect the change in position but can detect that in brightness of the interference wave.

✧ Detection principle of the anisotropy of light speed

There are two very important points to note. One is that the two beams join and go to the detection device, but not one beam through one slit and the other through another one. The combined mixed wave passes through both slits, that is, each beam passes through both slits. The second point is that they are trying to observe the difference in the frequency of the two beams. In modern experiments, instead of observing interference fringes using slits, two beams are combined and the difference in frequency is measured as the difference frequency (beat note frequency).

If there is a difference in the light speed between the two split beams that are emitted simultaneously, there will be a time difference Δt in the arrival at the junction. Because their mixed wave is measured, the two beams must arrive at the same time. Therefore, the light that takes Δt longer is emitted Δt earlier. There is hence a phase difference of $\omega\Delta t$ between the two beams at the detector. The displacement of the mixed wave of the two beams is expressed as below.

$$A_1 + A_2 = A\sin(kx - \omega t) + A\sin\big(kx - \omega(t + \Delta t)\big)\ , \qquad k = \omega/v \qquad (3)$$

Even if the light speeds in the two arms are different, since both beams are in the same direction from the half-mirror to the detector after they join, the light speed v is the same, and the angular frequency ω and wavenumber k are also the same for both beams. Here we devise to express the phase of A_1 as $0 = -\omega\Delta t/2 + \omega\Delta t/2$ and that of A_2 as $-\omega\Delta t = -\omega\Delta t/2 - \omega\Delta t/2$.

$$A_1 + A_2 = A\sin\left(kx - \omega t - \frac{\omega\Delta t}{2} + \frac{\omega\Delta t}{2}\right) + A\sin\left(kx - \omega t - \frac{\omega\Delta t}{2} - \frac{\omega\Delta t}{2}\right) \qquad (4)$$

The mixed wave above can be transformed as follows.

$$A_1 + A_2 = 2A\cos\frac{\omega\Delta t}{2}\sin\left(kx - \omega t - \frac{\omega\Delta t}{2}\right) \qquad (5)$$

This is the **interference wave in the detector** after the two beams join. This is a very important formula. When Δt changes due to a rotation of the apparatus by such as the rotation of the earth, it indicates the following results: (1) Even if Δt changes due to a rotation of the apparatus, the directions of the both beams are the same, so the light speed v, frequency ω, wavenumber k and wavelength are the same between the both beams. (2) The amplitude and phase of the mixed wave (interference wave) change with the change of Δt due to a rotation of the apparatus. As a conclusion, Michelson-Morley-like experiments cannot detect the change in spacing or position of interference fringes, but can detect the change in the brightness.

In fact, some phenomena suggesting the anisotropy of the light speed have been already mentioned. In the Michelson-Morley experiment, the interference fringes were unstable, and often dimmed or disappeared. They adjusted the mirrors to restore the image. They presumed that it was caused by noise by external factors such as vibration and temperature change. However, the main cause seems to be the change in the brightness due to the change in the phase difference between the two beams. A more direct example is the following. It was presented at a workshop (DICE) in

Italy in 2008 or 2010 that circadian variations in the information transfer speed were observed. In the transmission of information between a satellite, Chile and the East Coast of the US, the difference in the transmission speed between the points was observed to fluctuate with a period of one day. The graph of the circadian variation was really beautiful, and I immediately felt that this was exactly the data showing the anisotropy of the light speed. I asked the speaker "isn't it the light speed itself?", but he answered "it is not the light speed but a speed of information transmission". This transmission of information is performed by radio waves, and the transmission speed is equal to the propagation speed of electromagnetic waves (light).

2.2. Quantum mechanics

In 1924, de Broglie proposed the hypothesis that all particles, not just the light, have the wave-particle duality. He claimed that the de Broglie wave, later called as the matter wave, accompanies a particle. He claimed that the wave has the following relation like the light.

$$E = pv\,, \qquad E = \hbar\omega \quad \Rightarrow \quad p = \hbar k \tag{6}$$

The de Broglie hypothesis had a great impact, and the focus was on what the accompanying matter wave was in concrete and how it could be expressed. Heisenberg reported in 1925 a matrix equation for such waves using the condition $p = \hbar k$ of the de Broglie hypothesis, and Schrödinger reported a wave equation for that in 1926. The two were then proved to be mathematically equivalent, and give wave functions as a solution.

✧ Schrödinger equation

The de Broglie condition of Eq. (6) is applicable only for an energy quantum, which is the energy of one cycle.

$$E_q = E/\nu \tag{7}$$

However, Schrödinger chose the kinetic energy formula as the original equation.

$$E_k = \frac{1}{2}m_r v^2 = \frac{1}{2}pv = \frac{p^2}{2m_r} \tag{8}$$

To this he applied de Broglie condition, and got the **Schrödinger equation**.

$$i\hbar\frac{\partial}{\partial t}\psi(x,t) = -\frac{\hbar^2}{2m_r}\frac{\partial^2}{\partial x^2}\psi(x,t) \tag{9}$$

On the other hand, from the ECT, we reported the following **wave equation** instead of Schrödinger one.

$$i\hbar\frac{\partial}{\partial t}\psi(x,t) = -\frac{\hbar^2}{m_q}\frac{\partial^2}{\partial x^2}\psi(x,t)\,, \qquad m_q = E_q/c^2 \tag{10}$$

$E = pv$ is valid from Eq. (1) $E = Mv^2$ for any energy. However, $E_q = \hbar\omega = h\nu$ is valid only for an energy quantum. The mass m_q in the equation is that of an energy quantum.

The two wave equations are basically the same form with only difference in the mass; rest mass m_r or mass of energy quantum m_q. In the Schrödinger equation, m_r varies depending on individual particles. However, in reality the equation **should hold only for energy quanta** because it is derived from the relation of Eq. (6). The **mass m_r in the Schrödinger equation is a critical mistake**.

✧ Runaway of quantum mechanics

A solution of the both equations in general is the following wave function for plane waves.

$$\psi = A\exp\big(i(kx - \omega t)\big) \tag{11}$$

The standard quantum mechanics insists that a higher energy particle has a larger mass m_r and a greater frequency ω than those of a lower energy one. However, the ECT claims that both the mass m_q and the frequency ω are decided only by the linear velocity regardless the kind of particles (Ref.

[4]). For this type of wave equations, any linear combination of a solution is also a solution. From this aspect, they became to regard that the amplitudes of the solutions do not have a meaning, and any amplitudes and any combinations of them are possible. They brought the interpretation of wave functions as showing a probability of existence. Furthermore, they escalated to insist that not its solution but the equation is the essence of a physical property.

Thus, the standard quantum mechanics made a big mistake. It claimed that all solutions of the equation were possible as a desired matter wave. This conflicts with the mathematic principle that the converse is not necessarily true. When "the desired wave function is a solution of a certain wave equation" holds true, "a solution of the wave equation is the desired wave function" does not necessarily hold true. The set formed by the wave function solutions is a larger set that includes the set of the desired wave functions. Since they did not know a force that enables a vibration or circulation of energy, they got away by introducing the probability interpretation, which allowed to take numerous wave functions without a basis.

In the ECT, the wave function shows a distribution of the intrinsic energy of an elementary energy circulation. It is a circular motion if the particle is static, and becomes a helical motion if it is moving. The wave function is a solution of the wave equation, but its amplitude is limited to μ_0, which is the radius of the spacia (minimum unit of space, to be explained later).

2.3. Standard particle physics – gauge theory

The combination of such a wrong interpretation of the quantum mechanics and the gauge theory made the particle physics more chaotic.

✧ **Gauge theory**

When we express the state of a combination of particles as a matrix and seek the symmetry for a unitary transformation corresponding to a rotation of the matrix elements, it becomes necessary to introduce a field called a gauge field. In a gauge transformation, a force acts based on the gauge field, and the quantized gauge field is a gauge boson, which is the particle mediating the force. The electromagnetic force is said to be generated from the symmetry of the gauge transformation called U(1), and its gauge boson is said to be the photon. It is said that the SU(2) symmetry produces the weak force, whose mediating particles are three types of weak bosons, and that the SU(3) symmetry produces the strong force, whose mediating particles are gluons (8 types). The standard model of particles requires the symmetry of U(1)×SU(2)×SU(3), and tries to find a gauge field that satisfies the conditions for each gauge transformation, and express it in the form of Lagrangian.

✧ **Problems of the gauge theory**

The unitary group of each gauge transformation has its own unique algebra. In general, various groups have their own algebras that consist of their own axioms and operations. For instance, for the group representing all vectors, it is first necessary to define what a vector is, which becomes an axiom. Then, we will define the operations such as addition and product in the group. If an object satisfies the axioms, it can be regarded as a vector even if it does not look like at first glance, and the algebra of this group can be applied to it. However, in the gauge theory of particles, the group elements that represent elementary particles are not defined. Without a definition of the elements, the operations on them are being expanded. The wave function that is said to show the distribution of the existence probability of an elementary particle is not given, either. A composition of elementary particles is listed in a matrix, with 1 indicating that it is present and 0 indicating that it is not present, then the decays and interactions of particles are being developed. Things like particle creation operators and annihilation operators are introduced too conveniently.

The use of a unitary transformation algebra for undefined elements is **mathematically bankrupt**. Without specifying what kind of a particle they are, the 17 types of elementary particles are used as the elements of a particle composition. Treating them as an elementary one that cannot be broken down further, they escape to discuss their structure or origin.

Chapter 3: Intra-circulation and inter-circulation interactions

3.1. Energy circulation and intra-circulation force

✧ Energy circulation

The "**energy circulation**" here shall be what the intrinsic energy is distributed even and continuously on the circumference. We take the amount M of the intrinsic energy as the sum of local ones ΔM on the whole circumference ($d\Delta M/d\theta = 0$).

$$M = \int_0^{2\pi} \Delta M d\theta = \Delta M \int_0^{2\pi} d\theta = 2\pi\Delta M \tag{12}$$

We express the **energy distribution** by a wave function ψ. In the case of a circular motion, it becomes as follows, where μ is the radius, and ω is the frequency.

$$\psi = [X \quad Y] = [\mu\cos\omega t \quad \mu\sin\omega t] = \mu(\cos\omega t + i\sin\omega t) \tag{13}$$

Each local intrinsic energy has a phase θ as $\omega t + \theta$, but the intrinsic energy is expressed as a whole by taking the sum of $0 \le \theta \le 2\pi$. We use the **notation**, by which $\boldsymbol{E\psi}$ means that the energy E is distributed at ψ. The wave function ψ shows a common distribution (position of existence) not only for the total energy but for all such as the intrinsic energy and the momentum. They are expressed by a common wave function ψ as follows.

$$E\psi, \qquad M\psi, \qquad p\psi \tag{14}$$

The amount of the total energy can be expressed by the intrinsic energy and its circular velocity as follows.

$$E = M{V_c}^2 = M\mu^2\omega^2 \tag{15}$$

✧ Intra-circulation force

Next, let us consider the **intra-circulation force** that acts within an energy circulation. Let μ be the radius, and consider two local momentums $\mathbf{\Delta p_0}$ and $\mathbf{\Delta p_\theta}$ with the central angle θ apart on the circumference.

Fig. 2. Two local momentums on the circumference

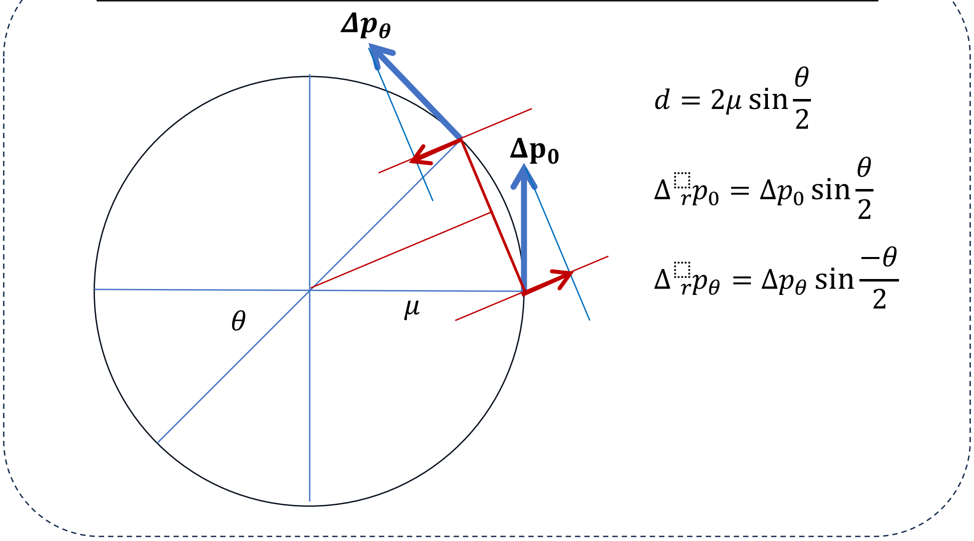

As shown in Fig. 2, the distance of the two local momentums (energies) is

$$d = 2\mu \sin\frac{\theta}{2}\ . \tag{16}$$

The force acting between $\mathbf{\Delta p_0}$ and $\mathbf{\Delta p_\theta}$ is given by the below formula.

$$\Delta F = K_f \frac{\Delta p_0 \Delta p_\theta}{d^2} \sin\frac{\theta}{2} \sin\frac{-\theta}{2} = -K_f \frac{\Delta p_0 \Delta p_\theta}{4\mu^2} \tag{17}$$

Remarkably, the angle θ and the distance d disappear from the formula, and the amount of the force is decided only by the radius of the circulation. The local momentum Δp_0 receives the following centripetal force from the momentum p of the whole circulation. The force in a tangential direction is set off each other to be zero.

$$cF_\perp = -K_f \frac{\Delta p_0}{4\mu^2} \int_0^{2\pi} \Delta p_\theta \sin\frac{\theta}{2} d\theta = -K_f \frac{\Delta p_0}{4\mu^2} \frac{p}{2\pi} 4 = -K_f \frac{p \Delta p_0}{2\pi\mu^2} \tag{18}$$

$$cF_{//} = -K_f \frac{\Delta p_0}{4\mu^2} \int_0^{2\pi} \Delta p_\theta \cos\frac{\theta}{2} d\theta = 0 \tag{19}$$

✧ **Radius of energy circulation**

If the intra-circulation force is balanced with the centrifugal force, it is a stable energy circulation. Consider an energy circulation, in which the intrinsic energy of M is circulating with the radius of r at the circulating velocity of V_c by the 2D expression. Since the formula of the centrifugal force by the mass is known, let us take the intrinsic energy m that moves at the light speed c by the 3D expression. m is moving helically with the main circular component V_c and the local circular component v_c.

$$E = MV_c{}^2 = m\left(V_c{}^2 + v_c{}^2\right) = mc^2 \tag{20}$$

On a local intrinsic energy Δm, the centrifugal force and the intra-circulation force balance and show the following relation from Eq. 18.

$$\frac{\Delta m V_c{}^2}{r} - K_f \frac{mV_c \Delta m V_c}{2\pi r^2} = 0 \tag{21}$$

$$2\pi r = K_f m$$

$$r = \frac{K_f}{2\pi} m = \frac{K_f}{2\pi c^2} E \tag{22}$$

As shown in Eq. (22), the **radius of an energy circulation is proportional to its energy**, and is independent of the circulating velocity.

3.2. Inter-circulation force between energy circulations

Let us examine a force working between two energy circulations. There are two types of working directions. The flat interaction is within the plane, and the orthogonal interaction is in the vertical direction to the plane. There are two cases of the relative circulating directions; same or opposite (conjugate).

✧ Flat interaction of opposite directions (conjugate pair)

Two energy circulations of the opposite frequencies form the coupled conjugate pair, which we also call as a double circulation. While this conjugate pair is internally attracted by a strong force, the vertical distance of the two circulations does not become zero, but as shown in Fig. 3, many **micro-circulations** are formed in the circumference direction and the vertical direction to it in a short distance. A coupled conjugate pair has a three-dimensional structure if the vertical direction is taken in account. When expressed in three dimensions, a coupled conjugate pair can be regarded as a series of many micro-circulations on the main circumference.

Fig. 3. Structure of a coupled conjugate pair and flat separation

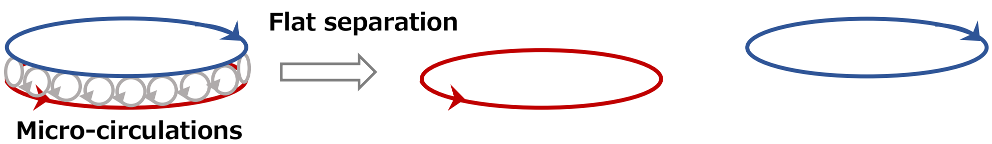

We call such a separation in the flat direction as shown in Fig. 3 as the "**flat separation**". Let us see the force working between them during the flat separation.

Consider a single circulation S of frequency ω and $\overline{S}$ of $-\omega$. We take the approximation to use the following two linear momentums orthogonal to the distance direction, which are apart by the distance of diameter. $\mathbf{e_r}$ is the unit vector for the orthogonal direction.

$$ {}_r p_h = \int_{-\pi/2}^{\pi/2} \Delta p \cos\alpha \, d\alpha = \frac{2}{\pi} p_h \tag{23} $$

$$ \mathbf{p_0}(S) \equiv {}_r p_h \mathbf{e_r} , \qquad \mathbf{p_\pi}(S) = -\, {}_r p_h \mathbf{e_r} \tag{24} $$

$$ \mathbf{p_0}(\overline{S}) \equiv -\, {}_r p_h \mathbf{e_r} , \qquad \mathbf{p_\pi}(\overline{S}) = {}_r p_h \mathbf{e_r} \tag{25} $$

As the distance, we use the relative value x to the diameter. Let x_0 be the relative diameter of the micro-circulations to the main one. With keeping the vertical distance as x_0, the two circulations slide horizontally. The local force in X between $\mathbf{p_0}(S)$ and $\mathbf{p_0}(\overline{S})$ is given by

$$F_x(p_0\overline{p_0}) = -K_f \frac{4{p_h}^2}{\pi^2} \frac{1}{4{\mu_0}^2} \frac{1}{x^2 + {x_0}^2} \frac{x}{\sqrt{x^2 + {x_0}^2}} = -K_f \frac{{p_h}^2}{\pi^2 {\mu_0}^2} \frac{x}{(x^2 + {x_0}^2)^{3/2}} . \quad (26)$$

The total force in X between the two circulations is as follows.

$$\boldsymbol{F_{flat}}(\boldsymbol{S} - \overline{\boldsymbol{S}}) = K_f \frac{{p_h}^2}{\pi^2 {\mu_0}^2} \left(\frac{x-1}{((x-1)^2 + {x_0}^2)^{3/2}} + \frac{x+1}{((x+1)^2 + {x_0}^2)^{3/2}} - \frac{2x}{(x^2 + {x_0}^2)^{3/2}} \right) \quad (27)$$

Let us express the constant part as Q_p and the variable part by x as $f_{flat}(x)$.

$$\boldsymbol{Q_p} \equiv K_f \frac{{p_h}^2}{\pi^2 {\mu_0}^2} \quad (28)$$

$$\boldsymbol{f_{flat}}(\boldsymbol{x}) \equiv \frac{x-1}{((x-1)^2 + {x_0}^2)^{3/2}} + \frac{x+1}{((x+1)^2 + {x_0}^2)^{3/2}} - \frac{2x}{(x^2 + {x_0}^2)^{3/2}} \quad (29)$$

Then, the force is expressed as

$$\boldsymbol{F_{flat}}(\boldsymbol{S} - \overline{\boldsymbol{S}}) = Q_p f_{flat}(x) . \quad (30)$$

The minus force is attractive in $x > 0$ and repulsive in $x < 0$. The potential energy is obtained by $U(x) = -\int F(x)dx + C$ as follows. We set $U(\infty) = 0$.

$$\boldsymbol{U_{flat}}(\boldsymbol{S} - \overline{\boldsymbol{S}}) = -\int Q_p f_{flat}(x)dx$$

$$= Q_p \left(\frac{1}{\sqrt{(x-1)^2 + {x_0}^2}} + \frac{1}{\sqrt{(x+1)^2 + {x_0}^2}} - \frac{2}{\sqrt{x^2 + {x_0}^2}} \right) \quad (31)$$

The force and potential energy are shown in Fig. 4. In $|x| < 1$, the force is attractive, working them to return to a coupled pair at $x = 0$. The potential energy shows a trough at $x = 0$. At $|x| = 1$, the force is zero, and the potential energy shows a crest. In $|x| > 1$, the force is repulsive and accelerates them to recede.

Fig. 4. Flat interaction of conjugated single circulations

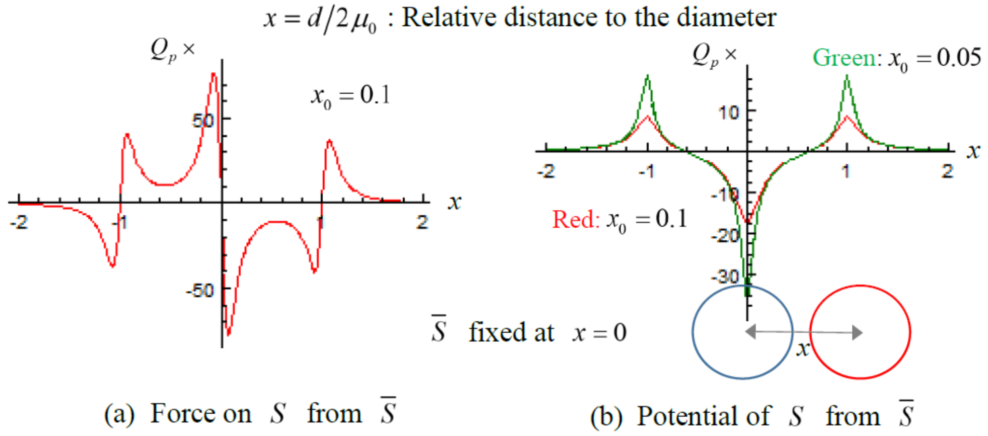

The force (a) and the potential energy (b) of conjugated two single circulations S and $\bar{S}$. The red lines are for $x_0 = 0.1$ and the green line is for $x_0 = 0.05$. x_0 is vertical distance (diameter of the micro-circulations).

The above equations and graphs are under the primary consideration for elementary circulations with the radius μ_0, but are applicable also to larger circulations.

✧ Flat interaction of same direction

While we will explain later, an energy circulation divides to two ones, then which separate. Let us see the flat interaction of two single circulations of the same circular direction.

Compared with the force between S and $\bar{S}$, signs of the components of the force between S and S are just reverse. Therefore, the force and the potential energy are the negative of those of S and $\bar{S}$.

$$\boldsymbol{F}_{flat}(\boldsymbol{S}-\boldsymbol{S}) = -F_{flat}(S-\bar{S}) = -Q_p f_{flat}(x) \tag{29}$$

$$\boldsymbol{U}_{flat}(\boldsymbol{S}-\boldsymbol{S}) = -U_{flat}(S-\bar{S}) \tag{30}$$

✧ Orthogonal interaction of opposite directions (conjugate pair)

As an example of opposite directions, let us see the orthogonal interaction of S and $\bar{S}$. The distance has the minimum value x_0, which is the diameter of micro-circulations. We take the range $x \geq x_0$. Take a minute local momentum $\Delta\mathbf{p}_\alpha$ on the circumference of S. Divide the circulating momentum of $\overline{S}$ to two halves; $\mathbf{p_0}$ and $\mathbf{p_\pi}$. Their directions are arc, but let us use the approximation treating them as linear, parallel or antiparallel to $\Delta\mathbf{p}_\alpha$, with the distance $2\mu_0$ (diameter of S). The magnitude of the linear momentums is the parallel component to $\Delta\mathbf{p}_\alpha$ and given as follows.

$$\int_{-\pi/2}^{\pi/2} \Delta p_0 \cos\beta \, d\beta = \int_{\pi/2}^{3\pi/2} \Delta p_\pi \cos\beta \, d\beta = \frac{2}{\pi} p_h \,, \qquad (p_h = p/2) \tag{31}$$

The force in the distance direction on $\Delta\mathbf{p}_\alpha$ of S from the whole circulation $\overline{S}$ is given as follows. x is the relative distance to the diameter $x = d/2\mu_0$.

$$F_x(\alpha) = K_f \Delta p_\alpha \frac{2p_h}{\pi} \frac{1}{4{\mu_0}^2} \left(\frac{x}{(x^2+1)\sqrt{x^2+1}} - \frac{1}{x^2} \right) \tag{32}$$

This force is common for any angle location α of S. We get the following force of the orthogonal interaction of S and $\overline{S}$.

$$\int_0^{2\pi} \Delta p_\alpha d\alpha = 2\pi \Delta p_\alpha = p = 2p_h \tag{33}$$

$$\boldsymbol{F_{ort}}(\boldsymbol{S} - \overline{\boldsymbol{S}}) = K_f \frac{{p_h}^2}{\pi {\mu_0}^2} \left(\frac{x}{(x^2+1)^{3/2}} - \frac{1}{x^2} \right) \tag{34}$$

The constant part is equal to Q_p expressed by Eq. (28) for the flat interaction. Let us express the variable part as $f_{ort}(x)$.

$$\boldsymbol{f_{ort}(x)} \equiv \frac{x}{(x^2+1)^{3/2}} - \frac{1}{x^2} \tag{35}$$

Then the force is expressed as below.

$$\boldsymbol{F_{ort}}(\boldsymbol{S} - \overline{\boldsymbol{S}}) = Q_p f_{ort}(x) \quad (x \geq x_0) \tag{36}$$

The potential energy is obtained by $U(x) = -\int F(x)dx + C$ as follows, with setting $U(\infty) = 0$.

$$\boldsymbol{U_{ort}}(\boldsymbol{S} - \overline{\boldsymbol{S}}) = Q_p \pi \left(\frac{1}{\sqrt{x^2+1}} - \frac{1}{x} \right) \quad (x \geq x_0) \tag{37}$$

✧ Orthogonal interaction of same direction

In the case of two circulations $(S-S)$ of the same circular direction, micro-circulations are not formed at a small distance, but the interaction of local circulations becomes notable. We will explain later the total features of the orthogonal interaction of main circulations and the flat interaction of local circulations in the session of the galactic seed separation. Here, we consider only the interaction of main circulations for the range $x \geq x_0$.

Signs of the force and potential energy are reverse to those of different directions $(S-\overline{S})$ as below. Q_p is given by Eq. (28).

$$\boldsymbol{F_{ort}(S-S)} = -F_{ort}\left(S-\overline{S}\right) = -Q_p f_{ort}(x) \quad (x \geq x_0) \tag{38}$$

$$\boldsymbol{U_{ort}(S-S)} = -U_{ort}\left(S-\overline{S}\right) = Q_p \pi \left(\frac{1}{x} - \frac{1}{\sqrt{x^2+1}}\right) \quad (x \geq x_0) \tag{39}$$

Chapter 4: Cosmic separation and space expansion

4.1. Cosmic separation

✧ Energy

We provide that the "energy" is a vibration in multiple (M) dimensions while we do not know the number M of dimensions. The same energy can be expressed in any number of dimensions depending on how the intrinsic energy is taken. If it is expressed in one dimension, the energy from motions in the rest M-1 dimensions shall act as the intrinsic energy, which is vibrating in one dimension. In order to vibrate in one dimension, a force is required. For providing this force, one additional dimension is necessary and the motion should become a circulation in two dimensions. In this case, energy is circulating by the centripetal force due to the fundamental force, and in any direction within the two-dimensional circular plane, it is vibrating one-dimensionally.

✧ Cosmic separation

Let us express the "**pre-cosmos**" before the expansion by M/2 pairs of 2D energy circulations. We provide that the pre-cosmos was symmetric in all dimensions. In order to be symmetric, each 2D circulation should bind to a circulation of opposite direction to form a **coupled conjugate pair**. While this conjugate pair is internally attracted by a strong force, the vertical distance of the two circulations does not become zero, but as shown in Fig. 3, many **micro-circulations** are formed in the circumference direction and the vertical direction to it in a short distance. A coupled conjugate pair has a three-dimensional structure if the vertical direction is taken in account. When expressed in three dimensions, a coupled conjugate pair can be regarded as a series of many micro-circulations on the main circumference.

When the width of the energy distribution of the pre-cosmos becomes larger than a threshold in any one-dimensional direction, the original amplitude in it cannot be maintained and it expands. Among the M/2 pairs, the coupled conjugate pair including this direction separates horizontally (flat separation) as shown in Fig. 3. Jointly with this separation, another coupled conjugate pair, the vertical direction of which is the prolonged one, separate orthogonally. We call it as the "**orthogonal separation**". In this way, the pre-cosmos divides into two universes. We call it as the "**cosmic separation**". We can express the cosmic separation as below, where μ is the radius and φ is a function to show a circulation.

$$E\mu_{pre}(\varphi_{12}\colon\varphi_{12}^{*}+\varphi_{34}\colon\varphi_{34}^{*})\longrightarrow\frac{E}{2}\mu_{u}(\varphi_{12}+\varphi_{34})+\frac{E}{2}\mu_{u}(\varphi_{12}^{*}+\varphi_{34}^{*}) \qquad (40)$$

$$\varphi=\exp(i\omega t)=\cos\omega t+i\sin\omega t\ ,\ \ \varphi^{*}=\exp(-i\omega t)$$

Fig. 5 shows its 3D image. In reality, the circulations are in the X_1-X_2 plane and in the X_3-X_4 plane, in total 4 dimensions. If the prolonged direction is X_1, the pair in X_1-X_2 separates horizontally, and the pair in X_3-X_4 separates orthogonally.

Fig. 5. 3D image of the cosmic separation in 4D space

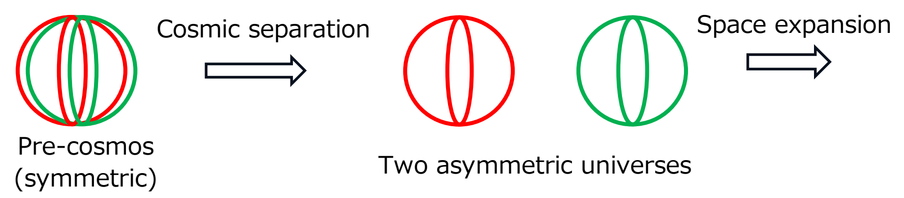

4.2. Space expansion

✧ Space expansion

In each separated universe, many local micro-circulations on the circumference of the pre-cosmos have been lost, the balance with the centrifugal force as one circulation breaks, then the space expansion in the 4 dimensions of the two circulations starts. We call it as the "**space expansion**". The remaining dimensions other than these four are called as the "**rest dimension**". A coupled conjugate pair in rest dimensions (e.g. X_5-X_6 plane) has the vertical direction of a rest dimension (e.g. X_7), and remains as the state of a coupled conjugate pair while the location in the expanded 4 dimensions separated to two universes. Even if the space expands, the radius keeps constant, and the circular momentums are set off each other to be zero. Since any directions in the rest dimensions are orthogonal to any directions in the 4D space, the circular energies there act as an intrinsic energy for motions in the expanding 4D space.

✧ Energy distribution of the universe

The two energy circulations (frequency ω) separated by the cosmic separation can be expressed in the 4D polar coordinates as below. Simultaneously with the cosmic separation, the space expansion starts, and the radius expands and the frequency decreases. However, for convenience, let us consider the state immediately after the separation.

$$\mathbf{X} = [\mu \quad \theta_1 \quad \theta_2 \quad \theta_3] = [\mu \quad \omega t \quad \theta_2 \quad \omega t] \tag{41}$$

Expressing it in the 4D cartesian coordinates, we get the below.

$$\mathbf{X} = \mu \begin{pmatrix} \cos\omega t + i\sin\omega t\cos\theta_2 + j\sin\omega t\sin\theta_2\cos\omega t \\ +k\sin\omega t\sin\theta_2\sin\omega t \end{pmatrix} \tag{42}$$

The imaginary units i, j, k are unit vectors of directions orthogonal each other and to the real part. Here, for the circulation of $\mu\theta_1$, we take the base vectors; $\mathbf{e_0}$ for the radius and $\mathbf{e_1}$ for the arc on the circumference.

$$\mathbf{e_0} \equiv \cos\theta_1 + i\sin\theta_1 \tag{43}$$

$$\mathbf{e_1} \equiv \cos(\theta_1 + \pi/2) + i\sin(\theta_1 + \pi/2) = i\mathbf{e_0} \tag{44}$$

The radius and the arc can be expressed as $\mu\mathbf{e_0}$ and $\mu\theta_1\mathbf{e_1} = \mu\omega t\mathbf{e_1}$. Jointly with j and k, $\mathbf{e_1}$ forms the 3D cartesian coordinates, in which Eq. (42) is expressed by the following formula.

$$\mathbf{X} = \mu\big(\omega t\mathbf{e_1}\cos\theta_2 + \sin\theta_2\,(j\cos\omega t + k\sin\omega t)\big) \tag{45}$$

✧ Space energy, apparent energy, and spacia

The cosmic energy, which shows the two energy circulations expanded in 4D, is distributed on the 3D surface of the 4D sphere (ball). We call the 3D surface as the "**space dimensions**" and the radius of the 4D sphere as the "**hidden dimension**". The width of the energy distribution in the hidden dimension H is very thin and invariant with the space expansion. Let $2\mu_0$ be this width, and treat the 4D sphere of the radius μ_0 as the minimum unit space. While the cosmic energy as a whole is circulating and asymmetric, we divide it into two parts; the symmetric one "**space energy**" and the asymmetric one "**apparent energy**". The space energy is distributed evenly in the whole space of the universe, and is a collection of coupled conjugate circulations. The circular momentums of the pair are set off each other to be zero, and the fundamental force does not act there. The space energy in the unit space of the radius μ_0 is named as the "**spacia**". The distribution and the amount of the spacia can be expressed as below.

$$E_\mu\psi_\mu = E_\mu\mu_0\big(\exp(i\omega_0 t) + \exp(-i\omega_0 t)\big) \tag{46}$$

$$\exp(i\omega_0 t) = \cos\omega_0 t + i\sin\omega_0 t$$

$$E_\mu = m_\mu {v_c}^2 = m_\mu {\mu_0}^2 {\omega_0}^2 = m_\mu c^2 \tag{47}$$

✧ Particle

An apparent energy is given as an additional circulation to one component of the coupled circulations of the spacia. This apparent energy can also be expressed as a vibration of the space energy as a medium. The circulation of an apparent energy shows the properties of a particle. An energy circulation can be static to the space energy, keeps a constant radius by the fundamental force, and interacts with others to exert an attractive or repulsive force. We can define the "**particle**" as an energy circulation.

We already explained the intra-circulation force in Section 3.1, and the inter-circulation force between two circulations in Section 3.2. Fig. 6 shows the image of the flat interaction of two energy circulations (particles). Two circulations with the same circular direction $+\omega$ shows a repulsive force when they overlap (left in Fig.6) and an attractive force when they are separated with no overlap (right). In the central state, where the two are adjacent, the force is zero, and this state is the most stable. In the case of opposite directions as $+\omega$ and $-\omega$, an attractive force acts at places from the overlapping state on the left to the adjacent state in the center, and they tend to return to the coupled conjugate pair (left). However, once they separate beyond adjacency, a repulsive force acts and they recede.

The state, in which two circulations of the same direction overlap (upper left in Fig. 6), comes up immediately after one energy circulation was divided to two. The two circulations make not only a **flat separation** but also an **orthogonal separation**.

Fig. 6. Flat interaction of energy circulations (within a plane)

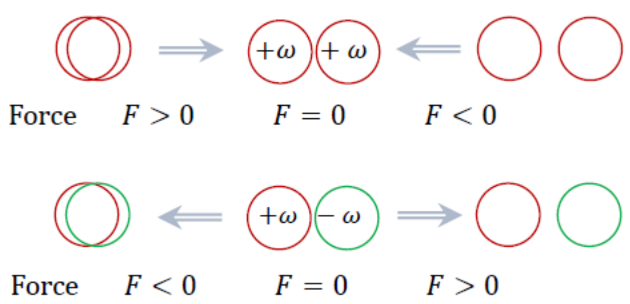

5.1. Early development of the universe

The distribution of the apparent energy in the 3D space immediately after the cosmic separation can also be expressed by Eq. (45). θ_2 is a parameter to show a location, and shows continuous values in the range of $0 \leq \theta_2 \leq \pi$.

Eq. (45): $\mathbf{X} = \mu\big(\omega t \mathbf{e_1} \cos\theta_2 + \sin\theta_2\,(j\cos\omega t + k\sin\omega t)\big)$

✧ **Cyclic decomposition**

The apparent energy immediately after the separation can no longer be maintained as a circulation as the space expands, and, as shown in Fig. 7, will make the separations and decompositions of energy circulations.

Fig. 7. Early development of the universe with space expansion

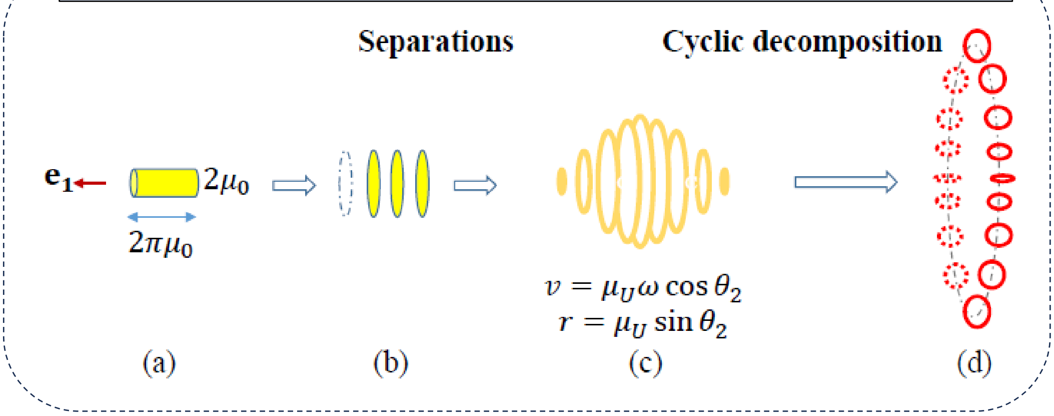

The both ends of the first state (a) are connected as circulating in the 4D space. It divides to multiple discs (b) due to the expansion, and each disc divides into multiple energy circulations (c). The radiuses of these circulations are proportional to $\sin\theta_2$, and the velocities in the $\mathbf{e_1}$ direction are proportional to $\cos\theta_2$. That is, in Fig. 7(c), they are moving leftward ($0 \leq \theta_2 \leq \pi/2$) and rightward ($\pi/2 \leq \theta_2 \leq \pi$). Then each circulation expands and decomposes all at once on the whole circumference to give a huge number of daughter circulations perpendicular to the parent one (d). We call it as the "**cyclic decomposition**". Although the ring distribution of the daughter circulations is not a continuum, intra-ring attractive forces due to the fundamental force act, and the **ring rotates by taking over the parent circulation**. Since this **ring of daughter circulations** is not a continuous energy circulation, its radius increases continuously by increasing distances between each other as the space expands.

✧ Asymmetric large-scale motions in the universe

As the space expands, the cyclic decompositions are repeated in many rounds, giving an infinite number of daughter circulations with much lower energies. As the energy value of an energy circulation decreases, the cyclic decomposition stops with it. We call those at this state as the "**galactic seed**". In this way, large-scale movements in the universe are shown, such as a galaxy cluster, in which galaxies gather in a ring and rotate, a supercluster, in which galaxy clusters gather in a ring and rotate, and the further rotation of gathered superclusters. Fig. 7(c) shows a set of circulations from only one disc. In fact, plural sets are overlapped.

Fig. 8. Large-scale distribution of superclusters

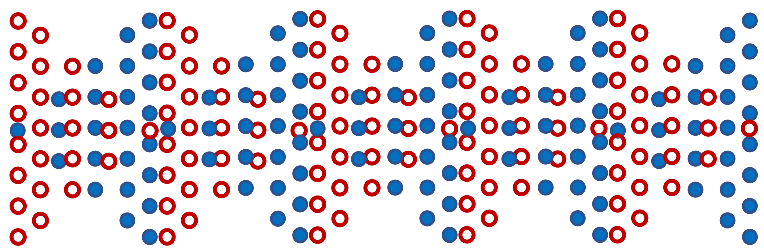

Each circle presents a ring of energy circulations, corresponding to a supercluster or larger cluster. The helicity of filled circles is left-handed and that of open circles is right-handed.

We show a rough image of distribution of energy circulations in Fig. 8, in which a filled circle has the left-handed helicity and an open circle has the right-handed one. Each circle there presents a cluster, supercluster or much larger cluster of galaxies.

In recent years, many large-scale motions and asymmetries of galaxies in the universe have been reported, but the existing standard model cannot explain them at all. For instance, Wang *et al*. reported that a cosmic filament has a spin, that is, galaxies are helically moving with a linear motion in the axis and a rotation around it. Shamir reported the asymmetric distribution of galactic spin directions. He demonstrated statistically significant dipole and quadrupole alignments of the spins for the whole universe. It suggested a rotation of the universe around a specific axis. Our model of cosmic evolution nicely meets these large-scale motions and should give them a theoretical basis.

5.2. Galactic seed separation

✧ Galactic seed division and separation

As mentioned in the section above, the countless galactic seeds were formed after many rounds of cyclic decomposition. Then, a galactic seed started to divide to two seeds, which separated each other. We call the process as the "**galactic seed separation**".

Fig. 9 show the galactic seed division and separation. The radius of an energy circulation is proportional to its energy amount as shown by Eq. (22). If a space-space dimensional energy circulation like a galactic seed is expressed in three space-dimensions, it has a donut-like shape. The intrinsic energy is in a **helical motion** with a **local circulation** and main one. The selected intrinsic energy is different between two-dimensional and three-dimensional representations.

Fig. 9. Galactic seed division and orthogonal separation

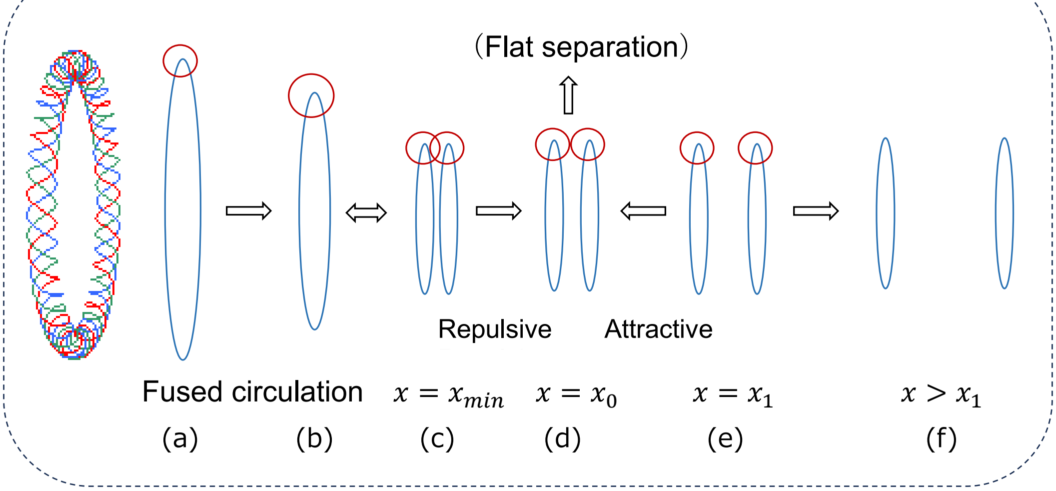

The red circle in Fig. 9 indicates one of local circulations of a galactic seed in the three-dimensional representation. The distribution of the speed to the main circulation and the local one is flexible, and varies depending on individual galactic seeds. Provided, there is a quantization condition that the frequency of the local circulation should be an integral multiple that of the main one, and the radius of the main circulation takes discrete values.

As the space expands, a galactic seed is releasing small energy circulations and radiations, and reducing its energy. By this reason, the radius of the main circulation decreases and that of local one increases to a new ratio (Fig. 9 (a)-(b)). As the local radius increases, it is divided into two galactic seeds as shown in Fig. 9 (b)-(c). Another reason to cause a galactic seed division is an extremely fast rate of the space expansion. In the early stages of the space expansion, the main radius increased slightly due to the rapid expansion, resulting in insufficient energy relative to the radius, and the galactic seed was divided as shown in Fig. 9. Such divisions occurred much more frequently in early stages.

Immediately after the galactic seed division, there works an interaction between local circulations in addition to that of main circulation. In the following section, let us see details on the force and potential energy in the galactic seed separation.

5.3. Force and potential energy in galactic seed separation

✧ Energy expression of a galactic seed

Take a galactic seed, in which the intrinsic energy M is circulating by the frequency Ω with the radius R in the 2D expression.

$$E = MV^2 = MR^2\Omega^2 \tag{48}$$

We can express the same galactic seed by the 3D expression as a helical motion of another intrinsic energy M_1 with the linear velocity V and the local circulating velocity V_c. Let μ be the radius and ω be the frequency of the local circulation.

$$E = M_1\left(V^2 + {V_c}^2\right) = M_1(R^2\Omega^2 + \mu^2\omega^2) = M_1{V_G}^2 \tag{49}$$

In the case of elementary circulations, as expressed by Eq. (20), the total velocity of the helical motion is the light speed c. However, the intrinsic energy M_1 is not moving at the light speed. Let V_G be the velocity, while it varies depending on individual galactic seeds. The linear motion makes the main circulation with R and Ω. The energy distribution is given as follows.

$$E\psi:\ \ \psi = jR\Omega t + \mu(\cos\omega t + i\sin\omega t) = [R\Omega t \quad \mu\cos\omega t \quad \mu\sin\omega t] \tag{50}$$

Since it is quantized as a continuous energy circulation, there is the following relation.

$$\omega = n\Omega\,, \qquad (n = \text{integer}) \tag{51}$$

The main radius R is proportional to the energy. Therefore, by a cyclic decomposition, **μ/R gets smaller**, and **ω/Ω gets larger**.

✧ Flat separation of galactic seeds

As an example, consider the separated two circulations with the following relations.

$$\mu/R = 0.1\,, \qquad \omega/\Omega = 4 \tag{52}$$

The function $f_{flat}(x)$ for $S-S$ shown by Eq. (29) is applicable for G-G of galactic seeds.

$$\text{Eq. (29):}\quad \boldsymbol{f_{flat}(x)} \equiv \frac{x-1}{((x-1)^2+{x_0}^2)^{3/2}} + \frac{x+1}{((x+1)^2+{x_0}^2)^{3/2}} - \frac{2x}{(x^2+{x_0}^2)^{3/2}}$$

Since the velocity V_G of galactic seeds is different from the light speed c, the force constant is different from that for $S-S$. Let us use $K_f(V_G)$.

$$K_f(V_G) \text{ for } V_G\,, \qquad \left(K_f \text{ for } c = \mu_0\omega_0\right) \tag{53}$$

We use the following variables and constant.

$$x \equiv d/2R\,, \qquad x_0 \equiv 2\mu/2R = \mu/R\,, \qquad P_h = \frac{1}{2}M_1V \tag{54}$$

The flat interaction force between the two galactic seeds is given as below.

$$\boldsymbol{F_{flat}(G-G)} = K_f(V_G)\frac{{P_h}^2}{\pi^2R^2}f_{flat}(x) \tag{55}$$

Here, let us define the constant Q_G as follows.

$$\boldsymbol{Q_G} \equiv K_f(V_G)\frac{{P_h}^2}{\pi^2R^2} \tag{56}$$

Then, the force is expressed as below.

$$\boldsymbol{F_{flat}(G-G)} = Q_G f_{flat}(x) \tag{57}$$

The potential energy is given by $U(x) = -\int F(x)dx + C$ as follows.

$$\boldsymbol{U_{flat}(G-G)} = Q_G\left(\frac{2}{\sqrt{x^2+{x_0}^2}} - \frac{1}{\sqrt{(x-1)^2+{x_0}^2}} - \frac{1}{\sqrt{(x+1)^2+{x_0}^2}}\right) \tag{58}$$

Fig. 10 shows the graphs of the force and potential energy in the flat separation of $G-G$, which are generated by a galactic seed division in Fig. 9 (b)-(c). x_0 is taken as $x_0 = \mu/R = 0.1$ as an example.

Fig. 10. Force and potential energy in the flat separation of divided two galactic seeds

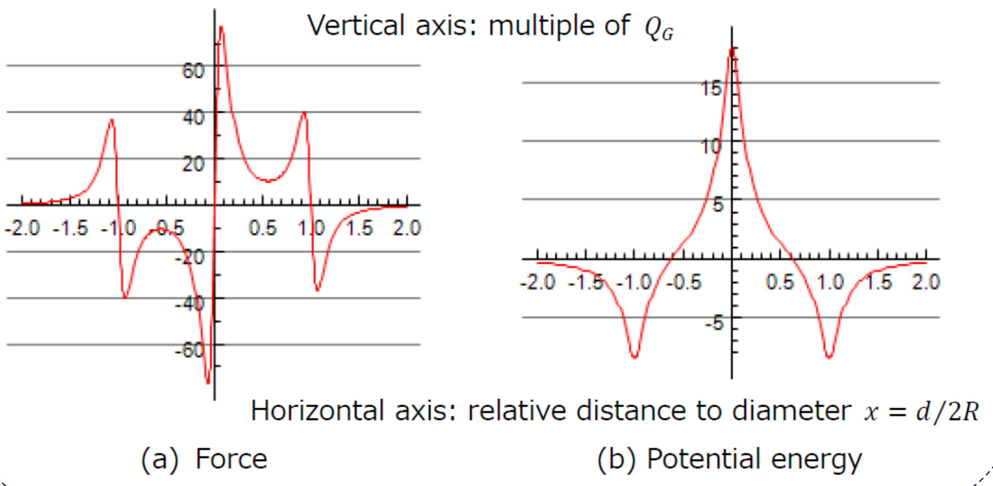

As we see in Eq. (58) and Fig. 10(b), the potential energy shows the trough at $|x| = 1$, where the two seeds tend to be attached.

✧ **Orthogonal separation of galactic seeds**

As shown in Fig. 9, the orthogonal separation included two interactions; that of main circulations and that of local circulations.

1) Orthogonal interaction of main circulations

The force function $f_{ort}(x)$ given by Eq. (35) is applicable for this case. With the force constant Q_G of Eq. (56), the force is given as below.

$$F_{ort}^{main} = Q_G f_{ort}(x) \tag{59}$$

2) Flat interaction of local circulations

The half momentum of the local circulation is given as follows.

$$P_h^{local} = \frac{1}{2} M_1 V_c = \frac{1}{2} M_1 V \frac{V_c}{V} = P_h \frac{\mu\omega}{R\Omega} \tag{60}$$

Use the distance parameter X as below (see Eq. (54)).

$$X \equiv \frac{d}{2\mu} = \frac{d}{2R}\frac{R}{\mu} = \frac{x}{x_0} \tag{61}$$

The force is given as follows.

$$F_{flat}^{local}(X) = Q_{flat}^{local}\left(\frac{2X}{\left(X^2 + {X_0}^2\right)^{3/2}} - \frac{X-1}{\left((X-1)^2 + {X_0}^2\right)^{3/2}} - \frac{X+1}{\left((X+1)^2 + {X_0}^2\right)^{3/2}}\right) \tag{62}$$

The force constant has the following relation to Q_G.

$$Q_{flat}^{local} = K_f(V_G)\frac{\left(P_h^{local}\right)^2}{\pi^2\mu^2} = K_f(V_G)\frac{{P_h}^2}{\pi^2 R^2}\left(\frac{\mu\omega}{R\Omega}\frac{R}{\mu}\right)^2 \tag{62}$$

From Eq. (56) of Q_G

$$Q_{flat}^{local} = Q_G\left(\frac{\omega}{\Omega}\right)^2 \tag{63}$$

Substitute Eq. (61) $X = x/x_0$ to the function.

$$f_{flat}^{local}(x) = \frac{2(x/x_0)}{\left((x/x_0)^2 + {X_0}^2\right)^{3/2}} - \frac{(x/x_0)-1}{\left(\left((x/x_0)-1\right)^2 + {X_0}^2\right)^{3/2}} - \frac{(x/x_0)+1}{\left(\left((x/x_0)+1\right)^2 + {X_0}^2\right)^{3/2}} \tag{64}$$

Then, the force is expressed as follows.

$$F_{flat}^{local} = Q_G\left(\frac{\omega}{\Omega}\right)^2 f_{flat}^{local}(x) \tag{65}$$

3) Total force in an orthogonal separation

The total force is given as below.

$$F_{ort}(G-G) = F_{ort}^{main} + F_{flat}^{local} = Q_G f_{ort}(x) + Q_G\left(\frac{\omega}{\Omega}\right)^2 f_{flat}^{local}(x) \tag{66}$$

As an example, let us use the following values:

$$x_0 = 0.1\,, \qquad X_0 = 0.1\,, \qquad \omega/\Omega = 4 \tag{67}$$

Finally, we get the force for the case as follows.

$$F_{ort}(G-G)=Q_G\pi\left(\frac{1}{x^2}-\frac{x}{(x^2+1)^{3/2}}\right)$$
$$+16Q_G\left(\begin{array}{c}\frac{20x}{((10x)^2+0.01)^{3/2}}-\frac{10x-1}{((10x-1)^2+0.01)^{3/2}}\\-\frac{10x+1}{((10x+1)^2+0.01)^{3/2}}\end{array}\right) \tag{68}$$

4) Potential energy of galactic seeds in an orthogonal separation

We get a potential energy by $U(x)=-\int F(x)dx+C$. From

$$\int x(x^2+a)^{-3/2}dx=-\frac{1}{\sqrt{x^2+a}}\,, \tag{69}$$

the integration of $f_{ort}(x)$ becomes

$$\int f_{ort}(x)dx=\int\pi\left(\frac{1}{x^2}-\frac{x}{(x^2+1)^{3/2}}\right)dx=\pi\left(\frac{1}{\sqrt{x^2+1}}-\frac{1}{x}\right). \tag{70}$$

Integration of $f_{flat}^{local}(x)$ by X is given as follows, where $X=x/x_0=10x$.

$$\int f_{flat}^{local}(x)dx=\int f_{flat}^{local}(x)dX\frac{dx}{dX}=0.1\int f_{flat}^{local}(x)dX \tag{71}$$

Finally, we get the following potential energy for this case.

$$U_{ort}(G-G)=-Q_G\pi\left(\frac{1}{\sqrt{x^2+1}}-\frac{1}{x}\right)$$
$$+1.6Q_G\left(\begin{array}{c}\frac{2}{\sqrt{(10x)^2+0.01}}-\frac{1}{\sqrt{(10x-1)^2+0.01}}\\-\frac{1}{\sqrt{(10x+1)^2+0.01}}\end{array}\right) \tag{72}$$

In Fig. 11, the graphs of the force expressed by Eq. (68) and the potential energy expressed by Eq. (72) for the orthogonal separation of galactic seeds are shown. Thus, we got the quantitative basis for the orthogonal separation of galactic seeds. Please have a look at Fig. 9 and Fig. 11 jointly.

Fig. 11. Force and potential energy in the orthogonal separation of divided two galactic seeds

Vertical axis: multiple of Q_G

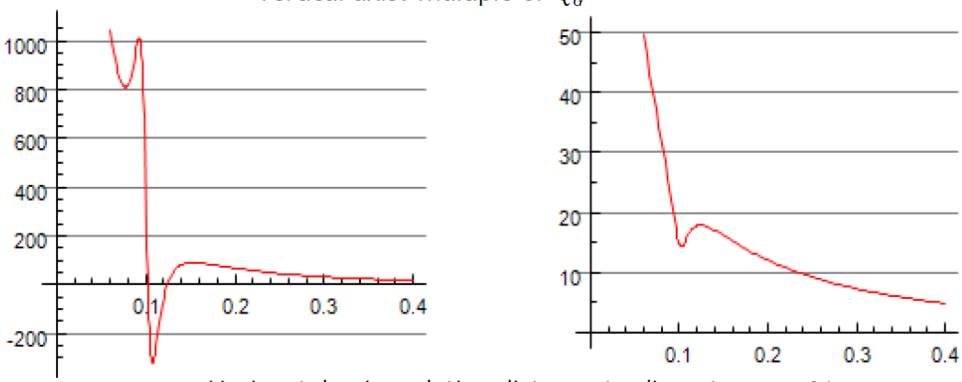

Horizontal axis: relative distance to diameter $x = d/2R$

(a) Force (b) Potential energy

5.4. Gamma-ray bursts and types of galactic seeds

✧ Release of potential energy in a galactic seed separation

The change in potential energy is incorporated in that of the intrinsic energy.

$$E = MV^2 = MV^2 - \Delta E_p + \Delta E_p = (M - \Delta M)V^2 + \Delta E \quad (73)$$

In a galactic seed separation, the decrease in potential energy is converted to the energy emission and the increase in kinetic energy.

$$E = (M - \Delta M)V^2 + \Delta E = (M - \Delta M)(V^2 + v^2) + \Delta E_e \quad (74)$$

The intrinsic energy M consists of various levels of energy circulations. The potential energy decrease happens simultaneously in all component circulations. Therefore, it shows rather a pulse-like emission of energy. There are two types of energy emission (radiation). One is the wave in hidden-space dimensions, that is, the **light**. The other is the wave in space-space dimensions, which is equal to so called the **gravitational wave**.

Space-space circulations are flexible in the ratio of the emission and the increase of linear velocity. Some circulations remain within the galactic seed and some are released as waves. Released gravitational waves move helically in the 3D space, and have a variety in the combination of the radius and the linear velocity. The smallest one is the neutrino, which has the same radius as that of the spacia. I do not think the name is proper, but leave it as the well-known "gravitational wave".

With respect to the light, we will explain in detail later, but please be noted that the intrinsic energy is vibrating in the hidden dimension and in a space dimension, and linearly moving to a space direction.

In the case of galactic seed separation, it releases a few pulse emissions of high energy, which we detect now as gamma-rays and gravitational waves, and the process is called as the **gamma-ray burst**.

✧ Pattern of galactic seed separation and resulting galactic seeds

As explained in Section 5.2, after the galactic seed division, primary orthogonal separation occurs. If the vertical speed is high enough, they continue to orthogonally recede. If the speed is slow, the seeds cannot pass over the energy crest, and return to the trough at $x = 0.1$ in Fig. 11, from where they start the flat separation.

Fig. 12. Potential energy in galactic seed separations

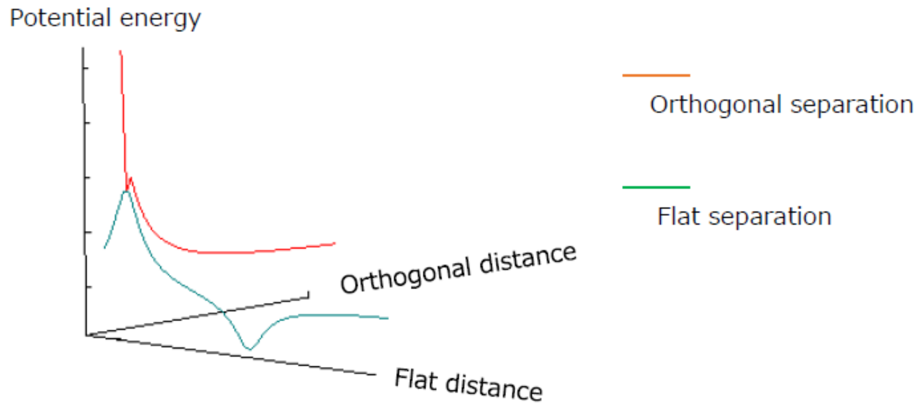

Fig. 12 is the combined graphs of the potential energy in the orthogonal separation and that in the flat separation. There are roughly three types of resulting galactic seeds.

Type-1 galactic seeds:

- Orthogonal – orthogonal separation
- Continue to recede.
- Result in two **isolated single** galactic seeds.

Type-2 galactic seeds:

- Orthogonal – flat separation
- High speed at the trough of flat separation, then stop. The distance keeps nearly constant.
- Result in **rotating binary** galactic seeds.

Type-3 galactic seeds:

- Orthogonal – flat separation
- Not enough speed at the trough of flat separation. They vibrate there, lose energy by bremsstrahlung, then attach together.
- Result in **two attached** galactic seeds. Rotating or non-rotating.

Depending on the above cases of galactic seed separation, various types of gamma-ray bursts come out. An energy emission by a decrease in potential energy is made as a pulse. In the Type-3, the seeds vibrate around the energy trough, and their energies gradually decrease by radiating light, which is continuous and called as bremsstrahlung. This light radiation is the afterglow associated with the class of long GRBs. Then they attach together with or without rotation mutually.

Chapter 6: Formation of a galaxy

6.1. Stellar seed release from a galactic seed

Once the energy of a galactic seed decreases to a certain level, a further galactic division-separation becomes impossible. Gamma-ray bursts do not occur from this timing. Then, releases of stellar seeds from the galactic seed begin. The "**stellar seed**" is the daughter energy circulation from the galactic seed. There are two kinds of stellar seed release; the linear release and the ring release.

✧ Linear release of stellar seeds

A stellar seed is release from a local circulation of a galactic seed as shown in Fig. 13(a). The **linear releases** occur one by one and randomly from various local circulations. The release direction is flat or orthogonal to the plane of galactic seed, or intermediate. The **flat release** is to the tangential direction within the plane. A stellar seed moves linearly in the flat and intermediate releases, since it basically does not receive the fundamental force from other stellar seeds or the galactic seed. Cumulation of flat and intermittent releases forms an **elliptical galaxy** or **halo** structure.

On the other hand, a stellar seed by the **orthogonal release** firstly moves jointly with the galactic seed, but receives a repulsive force from the nearby part of the galactic seed. As shown in Fig. 13(b), it spirally moves to the center and get static over or beneath the center. Cumulation of many stellar seeds released orthogonally over long time with the space expansion forms the **bulge** structure as shown in Fig. 13(b).

Fig. 13. Linear releases of stellar seeds

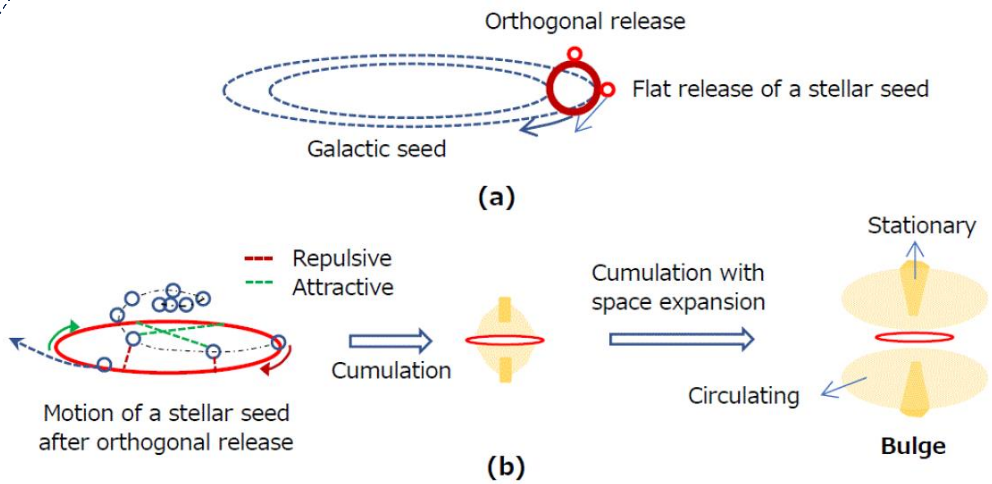

Flat and intermediate releases → form an **elliptical galaxy** or **halo**
Orthogonal releases → form a **bulge** structure

✧ Ring release of stellar seeds

As the space expands, a galactic seed cannot expand its radius since it is a continuum. Not only random linear releases mentioned above, stellar seeds are released simultaneously on the whole circumference. We may also regard it as that a small outer part of the galactic seed separates from the main part, and then it decomposes to daughter circulations by the cyclic decomposition. We call it as the "**ring release**". A ring release happens intermittently, gives a distribution of stellar seeds in a ring.

Many ring releases for long time gives a distribution of multiple concentric rings of stellar seeds, which is a **disc of galaxy**. A very important property of a stellar seed ring is that the fundamental force works between stellar seeds and they **continue to circulate**. While the ring is not a continuum, but there works the **intra-ring force**, which results in a centripetal force on each stellar seed.

✧ Circulating velocity of stars in a galactic disc

The orbiting speed of stars composing a galactic disc is almost same at any radial distances. According to the standard cosmology, it is regarded that a star is orbiting with the balance of the centrifugal force and the gravitational attraction, and that the square of the velocity is inversely proportional to the radius.

$$m\omega^2 r - G\frac{Mm}{r^2} = 0\,, \qquad v^2 r = GM \tag{75}$$

The rotation velocity of a galactic disc is one of the most important mysteries, and it is expected that unknown dark matter exists in the halo surrounding the disc. However, in fact, the centripetal force is not the gravity but the intra-ring force by the fundamental force.

As the space expands, the moving speed in the 3D space does not change. Therefore, the circulating velocity of a ring of stellar seeds does not change from the initial speed as the space expands, while the radius of the ring expands.

The release of a stellar seed ring from a galactic seed is a division of the intrinsic energy as shown below. So, the circulating velocity does not change before and after the release.

$$E = M_0 {V_G}^2 \;\longrightarrow\; E = (M_1 + M_2){V_G}^2 \tag{76}$$

By repeating a release of a stellar seed ring, the radius of the galactic seed gets smaller due to the decrease of energy, but its circulating velocity does not change. Therefore, whenever a ring of stellar seeds is released, the circulating velocity is the same for any rings. It results in the fact that the orbiting speed of stars (matters) in a galactic disc is almost constant at any radial distances from the galactic center. In conclusion, **dark matter does not exist**.

The intra-ring force is not balanced with the centrifugal force. Therefore, the ring radius gradually increases. However, due to the large value of the radius, its increase is negligible compared with the space expansion. Fig. 14 shows a simulation of the path of a stellar seed since released from a galactic seed 4 billion years after the cosmic separation to the present (13.7 billion years). v is the circulating velocity per 100 million years. r_0 is the radius of the galactic seed when the stellar seed was released. As we see there, if the angular velocity of the galactic seed is high, a stellar seed in a ring firstly shows a circular motion, then gradually becomes spiral, but its circulating velocity is constant all the way.

Fig. 14. Motion of stellar seed after ring release

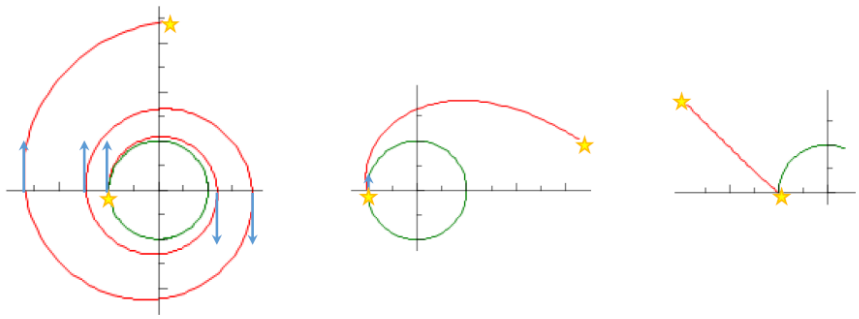

(a) $v = 0.5\, r_0$ (b) $v = 0.1\, r_0$ (c) $v = 0.02\, r_0$

From $x = 40$ to $x = 137$

6.2. Simulation of galaxy formation

Depending on the three types of the galactic seeds, and linear or ring releases of stellar seeds, various shapes of galaxies are formed. Let us simulate the galaxy formation.

For simulation, we use an **exponential time unit**. For $T_{1.1} = m$, the space expands by 1.1^m times. The present is $m = 0$. The length r_m at $T_{1.1} = -m$ expands to r_0 at present $T_{1.1} = 0$.

$$r_m : \text{ length at } T_{1.1} = -m \tag{77}$$

$$r_0 : \text{ present length at } T_{1.1} = 0\,, \qquad r_0 = 1.1^m r_m \tag{78}$$

We assume that the ring releases of stellar seeds occur intermittently once per $T_{1.1} = 1$.

$$\text{Ring releases: happen once per } T_{1.1} = 1 \tag{79}$$

This interval was seen in 42 reported shells of NGC 3923.

As a **unit of distance**, let one be the radius of a galactic seed, while it varies among individual seeds. As the space expands, we basically treat the galactic seed radius be constant except for some cases.

$$r_G \equiv 1 \quad (\text{galactic seed radius}) \tag{80}$$

The stellar seed here includes any generations of a stellar system in its development; stellar seed, star, supernova, reformed stellar seed with interstellar matters and re-born star. In general, stellar seeds by a linear release have a small energy, and still appear as a first-generation star. They are old stars without new-star formation. On the other hand, stellar seeds by a ring release have a high energy, and have experienced a few rounds of star-generation, supernova explosion and re-generation of star. We will not care of this stellar seed cycle for discussing the distribution of stellar seeds onward.

✧ Single galactic seed – linear releases (Type 1-1)

In the case of linear releases from a single galactic seed, stellar seeds are released 3D-radially and rather randomly, and move linearly at a uniform speed same as the circulating velocity of the galactic seed. It forms an **elliptical galaxy** (Type 1-1). A very important feature of this type is that stellar seeds are not circulating but linearly moving

✧ Single galactic seed – ring releases (Type 1-2)

If the energy and the angular velocity are high enough, a ring release of stellar seeds occurs. Since a released ring of stellar seeds is not a continuum, it expands as the space expands while the seeds continue to circulate in a ring. As an example of simulation, a ring of stellar seeds is released once every $T_{1.1} = 1$ from a single galactic seed. The release started at $T_{1.1} = -24$ and continues to the present $T_{1.1} = 0$.

To express a ring, we use one circle as below, where R_m is the radius of the ring at $T_{1.1} = -m$.

$$[x_m, y_m] = R_m[\sin t, \cos t] = 1.1^m[\sin t, \cos t] \quad (0 \le t \le 2\pi) \qquad (81)$$

Fig. 15. Ring releases from a single galactic seed

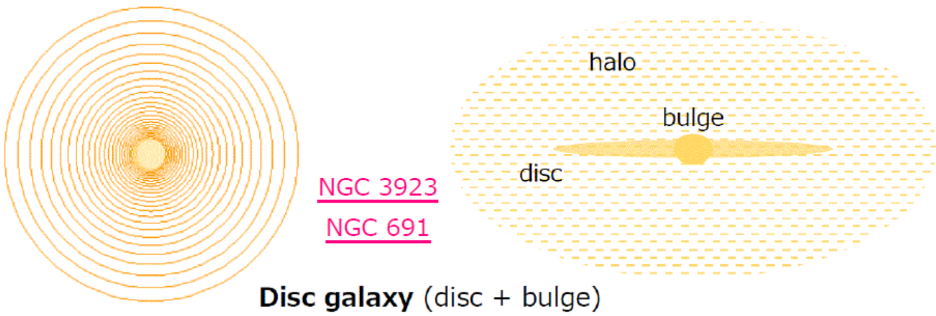

Disc galaxy (disc + bulge)

(a) Intermittent ring releases once per $T_{1.1} = 1$ ($T_{1.1} = -24$ to 0)
$[x_m, y_m] = R_m[\sin t, \cos t], R_m = 1.1^m \quad (0 \le t \le 2\pi)$ ($m = 0$ to 24)

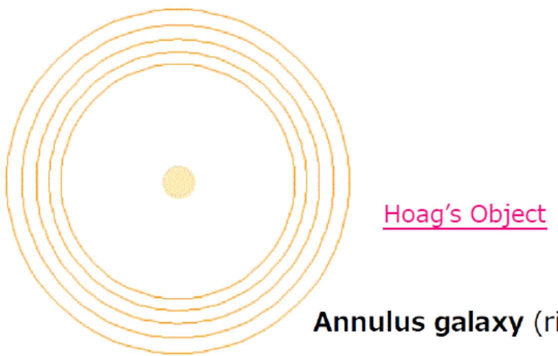

Annulus galaxy (rings+ bulge)

(b) Galactic seed released rings then exhausted ($T_{1.1} = -26$ to -22).

Fig. 15(a) shows the sum of rings from $m = 0$ to $m = 24$, that is, from $T_{1.1} = -24$ to $T_{1.1} = 0$. We named this type as the "**disc galaxy**" (Type 1-2). Other than ring releases, linear releases also occur, and form a bulge and a halo. A typical example of a disc galaxy is NGC 3923, which is generally classified as an elliptical shell galaxy. NGC 691 is another example.

In the standard cosmology, even this simple disc galaxy cannot be explained why and how such a thin disc is formed while dark matter is distributed spherically in the halo region. Only from the gravitational force, it is impossible to simulate the formation of galaxies.

If the galactic seed exhausted on the way of ring releases, it forms an annulus pattern of rings with a void inside and a bulge at the center. Fig. 15(b) is a simulation with the conditions: once per $T_{1.1} = 1$ ring release from $T_{1.1} = -26$ to $T_{1.1} = -22$, at which time the galactic seed disappeared due to exhaustion of energy. We call this type of galaxies as the "**annulus galaxy**" while generally called as a ring galaxy. An example of this type is the Hoag's Object. Its structure is in an excellent agreement with the simulated results whereas the standard cosmology leaves the galaxy's details mysterious. This class is different from a barred ring galaxy, which we will show later.

✧ Rotating binary galactic seeds – ring releases (Type 2-1)

Next, let us consider the ring releases form rotating binary galactic seeds. We treat the radius of galactic seeds constant, but the distance of two seeds expands as the space expands.

Let us take the following conditions: The initial radius of the binary rotation of galactic seeds at $T_{1.1} = -18$ is $R_{18} = 3$. The seeds rotate by the initial angular velocity $\Omega_{1.1}(-18) = \Omega_{18} = \pi/8$, and release a ring of stellar seeds once every $T_{1.1} = 1$ from $T_{1.1} = -18$ to $T_{1.1} = 0$.

The radius of the binary rotation increases as the space expands, given by

$$R_m = 3 * 1.1^{18-m} . \quad (82)$$

The angular velocity decreases as shown below.

$$\Omega_m = \Omega_{18}\frac{R_{18}}{R_m} = \frac{\pi}{8}\cdot\frac{3}{3*1.1^{18-m}} = \frac{\pi}{8}\cdot\frac{1.1^m}{1.1^{18}} \quad (83)$$

The angular phase of the location of a galactic seed becomes as below, where set as $\theta_0 = 0$.

$$\theta_m = \int_0^m \Omega_m \, dm = \frac{\pi}{8*1.1^{18}}\frac{1.1^m - 1}{\log 1.1} \approx \frac{\pi(1.1^m - 1)}{8*5.56*0.0953} \approx 0.236\pi(1.1^m - 1) \quad (84)$$

The locations of the galactic seeds at $T_{1.1} = -m$ from $m = 18$ to $m = 0$ (present) are given as follows and shown in Fig. 16(a).

Galactic seeds in Fig. 16(a):

$$[x_m, y_m]_1 = [\sin t + R_m \cos\theta_m\,,\ \cos t + R_m \sin\theta_m] \quad (84)$$

$$[x_m, y_m]_2 = [\sin t - R_m \cos\theta_m\,,\ \cos t - R_m \sin\theta_m] \quad (85)$$

$$r = 1\,, \qquad R_m = 3*1.1^{18-m}\,, \qquad \theta_m = 0.236\pi(1.1^m - 1) \quad (86)$$

$$m = 0 \text{ to } 18$$

A ring of stellar seeds is released once every $T_{1.1} = 1$. If the galactic seeds rotate binarily, a released ring stays there and depart from the galactic seed. By the space expansion, its location from the center prolongs and is now on the circle, on which the galactic seeds are currently located, as shown in Fig. 15(a). The radius of a released ring also expands by the space expansion. The current distributions of released rings are shown in Fig. 15(a) and given as follows.

Current distributions of released rings in Fig. 16(a):

$$[x_m, y_m]_1 = [r_m \sin t + R_0 \cos\theta_m\,,\ r_m \cos t + R_0 \sin\theta_m] \quad (87)$$

$$[x_m, y_m]_2 = [r_m \sin t - R_0 \cos\theta_m\,,\ r_m \cos t - R_0 \sin\theta_m] \quad (88)$$

$$r_m = 1.1^m\,, \qquad R_0 = 3*1.1^{18} \approx 16.7\,, \qquad \theta_m = 0.236\pi(1.1^m - 1) \quad (89)$$

$$m = 0 \text{ to } 18$$

Fig. 16. Ring releases from rotating binary galactic seeds

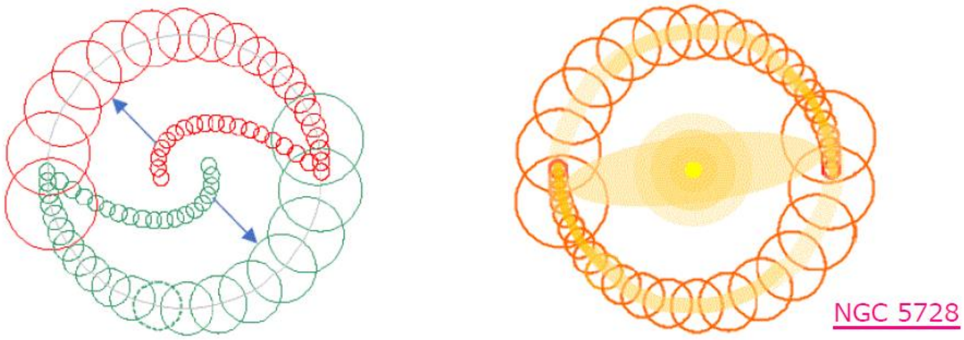

(a) Intermittent ring releases (b) **Barred ring galaxy**

$$T_{1.1} = -18 \text{ to } 0: r_m = 1.1^m.\ R_0 = 3 * 1.1^{18},\ \theta_m = 0.236\pi(1.1^m - 1)$$

$$R_m = 3 * 1.1^{18-m}\ ,\quad m = 0 \text{ to } 18$$

Galactic seeds:
$$[x_m, y_m]_1 = [\sin t + R_m \cos\theta_m\,, \cos t + R_m \sin\theta_m]$$
$$[x_m, y_m]_2 = [\sin t - R_m \cos\theta_m\,, \cos t - R_m \sin\theta_m]$$

Released rings:
$$[x_m, y_m]_1 = [r_m \sin t + R_0 \cos\theta_m\,, r_m \cos t + R_0 \sin\theta_m]$$
$$[x_m, y_m]_2 = [r_m \sin t - R_0 \cos\theta_m\,, r_m \cos t - R_0 \sin\theta_m]$$

By orthogonal releases, a **bulge** is formed (Fig. 13(b)). However, it departs from the galactic seed because the seed rotates binarily. Like a released ring, a bulge is now located on the circle of the current location of the galactic seeds. Once departed from the galactic seed, the circulating part of the bulge can no longer keep circulation, but scatters to outside. Only the stationary core part remains. We roughly regard the **radius of the core part as 0.3 times** that of a released ring. The ring releases are intermittent, but the bulge formation is rather continuous. The current distribution of the bulge is a continuous circle as shown in Fig. 16(b).

Furthermore, a **bar-bulge** is also formed, which will be explained in the next paragraph. Fig. 16(b) is the total figure of this type including released rings, bulge and bar-bulge, which we named as the "**barred ring galaxy**" (Type 2-1). A typical example is NGC 5728.

✧ **Bar-bulge**

The event of a ring release is rather seldom only once per $T_{1.1} = 1$. Independent linear releases of stellar seeds occur quite frequently. Released seeds form the halo. Seeds by flat release move in the tangential direction at each point of the circumference. In the special direction, where the motion from one galactic seed meets in antiparallel with that from the other one, two streams of stellar seeds make a circulation as shown in Fig. 17(a). By cumulation and the space expression, a circulating cluster of stellar seeds is formed. We named it as the "**bar-bulge**". Since the two galactic seeds have been rotating, the current distribution of a bar-bulge is shifted to the left a little in case of a right rotation as shown in Fig. 17(b).

Fig. 17. Formation of a bar-bulge

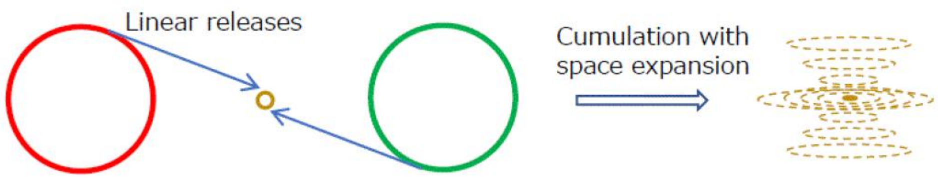

(a) Formation of a "**bar-bulge**" of stellar seeds

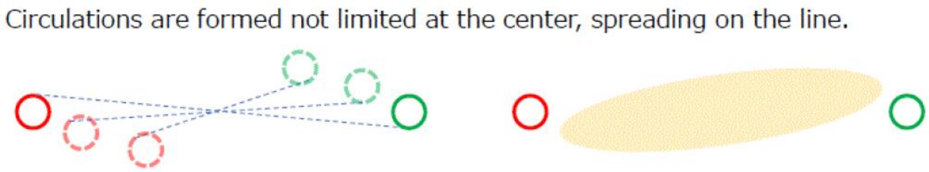

(b) Distribution of **bar-bulges**

✧ **Rotating binary galactic seeds – linear releases from binary ends (Type 2-2)**

If the rotating speed of the binary galactic seeds is high, stellar seeds are released from the two binary ends of the galactic seeds instead of a ring release, and move linearly. The simulation is shown in Fig. 18(a). The grey circles there present a distance circle from the binary end, where a stellar seed was released, for each time $T_{1.1} = -m$. The stellar seed linearly moves in the tangential direction. The **crossing point** of the **distance circle** and the **tangential line** is the location where the seed exists now. In Fig. 18(a), we manually plotted the crossing points by an orange circle. Between two plots, there exist more stellar seeds almost continuously. The series of plots in green-yellow circles are those released from the other galactic seed. Fig. 18(a) is under the following conditions:

- Linear releases from two binary ends occurred from $T_{1.1} = -16$ to $T_{1.1} = 0$. Due to the decrease of the angular velocity $\Omega_{1.1}$, linear releases from binary ends would stop, but let treat it to continue to the present in this simulation.
- The initial radius of binary rotation of galactic seeds is $R_{16} = 3$ at $T_{1.1} = -16$. The linear velocity of the released stellar seed is $V_{1.1} = 1.2$, which is invariant by the space expansion.
- The initial angular velocity of the rotation of galactic seeds is $\Omega_{1.1}(-16) = \pi/6$. By the space expansion, it decreases.

The angular velocity and the phase of the location of the galactic seed are given as follows.

$$\Omega_m = \Omega_{16}\frac{R_{16}}{R_m} = \frac{\pi}{6}\cdot\frac{3}{3 * 1.1^{16-m}} = \frac{\pi}{6}\cdot\frac{1.1^m}{1.1^{16}} \tag{90}$$

$$\theta_m = \int_0^m \Omega_m \, dm = \frac{\pi}{6 * 1.1^{16}}\frac{1.1^m - 1}{\log 1.1} \approx \frac{\pi(1.1^m - 1)}{6 * 2.853 * 0.0953} \approx 0.613\pi(1.1^m - 1) \tag{91}$$

The locations of the galactic seeds at $T_{1.1} = -m$ are given as below.

Galactic seeds in Fig. 18(a):

$$[x_m, y_m]_1 = [\sin t + R_m \cos\theta_m\,,\ \cos t + R_m \sin\theta_m] \quad (92)$$

$$[x_m, y_m]_2 = [\sin t - R_m \cos\theta_m\,,\ \cos t - R_m \sin\theta_m] \quad (93)$$

$$r = 1\,, \qquad R_m = 3 * 1.1^{16-m}\,, \qquad \theta_m = 0.613\pi(1.1^m - 1) \qquad (94)$$

$$m = 0 \text{ to } 16$$

The moved distance of a stellar seed is $V_{1.1}T_{1.1} = 1.2m$. However, it prolongs by the space expansion. If the space is expanded by n times, the present distance PD of a moved distance vt is given by the following formula, which will be explained in the Section 8.4 as Eq. (183).

$$PD = \frac{2n}{n+1}vt \qquad (95)$$

The distance circle of a stellar seed, which was released at $T_{1.1} = -m$, is given as follows.

Distance circles of released stellar seeds in Fig. 18(a):

$$[x_m, y_m]_1 = [r_m \sin t + (R_m + 1)\cos\theta_m\,,\ r_m \cos t + (R_m + 1)\sin\theta_m] \quad (96)$$

$$r_m = 1.2m\frac{2 * 1.1^m}{1.1^m + 1}\,, \qquad R_m = 3 * 1.1^{(16-m)}\,, \qquad \theta_m = 0.613\pi(1.1^m - 1) \qquad (97)$$

$$m = 0 \text{ to } 16$$

Fig. 18(a) shows crossing points of the distance circles with the respective tangential lines as well as those for released seeds from the other galactic seed. Fig. 18(b) is the overall appearance including the bar-bulge. Let us call this type of galaxies as the "**barred arm galaxy**”. A typical example of this type is NGC 1300, which is usually classified as a barred spiral galaxy.

Fig. 18. Linear releases from binary ends of rotating binary galactic seeds

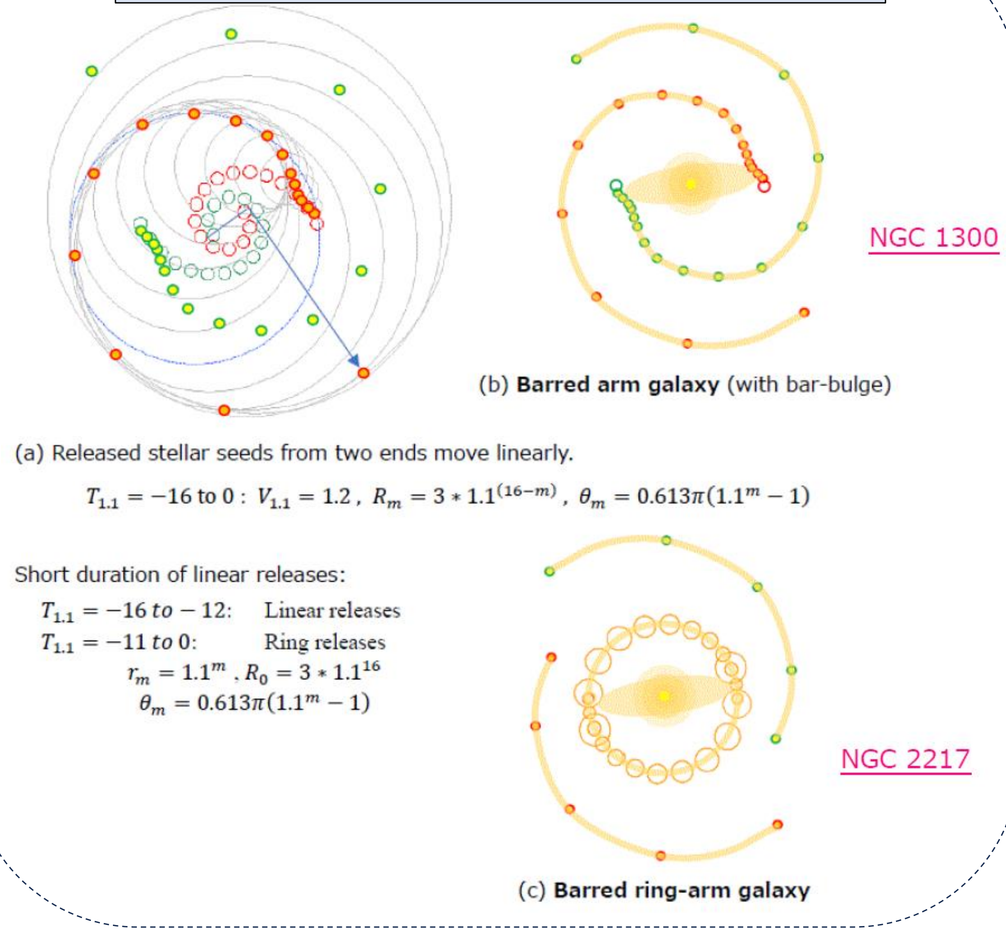

If the linear releases from binary ends stop and the ring releases start early, it becomes close to a barred ring galaxy shown in Fig. 16(b). Fig. 18(c) is for the case of the linear releases from $T_{1.1} = -16$ to $T_{1.1} = -12$ and the ring releases from $T_{1.1} = -11$ to $T_{1.1} = 0$. Let us call this type as the "**barred ring-arm galaxy**". NGC 2217 is an example of this one.

✧ Two attached galactic seeds – ring releases (Type 3-1)

Ring releases occur from two attached galactic seeds. Overlapping the two discs from two sources, there appears a pattern of difference in the intensity of stellar seeds. In many cases, the attached two galactic seeds rotate, but there is a variety of the rotating velocity. Fig. 19 shows patterns of resulted stellar seeds for respective values of the angular velocity $\Omega_{1.1}$ per $T_{1.1} = 1$ from $T_{1.1} = -24$ to $T_{1.1} = 0$.

Current distributions of released rings in Fig. 19:

$$[x_m, y_m]_1 = [r_m \sin t + \cos(m\Omega_{1.1}),\ r_m \cos t + \sin(m\Omega_{1.1})] \quad (98)$$

$$[x_m, y_m]_2 = [r_m \sin t - \cos(m\Omega_{1.1}),\ r_m \cos t - \sin(m\Omega_{1.1})] \quad (99)$$

$$r_m = 1.1^m, \qquad \Omega_{1.1} = 0\ (a), \frac{\pi}{12}\ (b), \frac{\pi}{8}\ (c), \frac{\pi}{6}\ (d) \text{ or } \frac{\pi}{4}\ (e) \qquad (100)$$

$$m = 0 \text{ to } 24$$

As shown in Fig. 19, spiral arms appear more significantly as the rotating angular velocity $\Omega_{1.1}$ gets larger. Let us collectively call these galaxies by ring releases from attached two galactic seeds as the "**double-disc galaxy**" (Type 3-1).

Fig. 19 (a) is the case that two galactic seeds do not rotate. The resulted galaxy does not have a clear spiral arm. An example of this non-rotating type is the Andromeda Galaxy. Its visible-light image seems close to a uniform single disc at glance, but there are two discs which are shifted a little from a single plane. Its pictures in infrared, blue-white or ultraviolet show clear rings of different centers. Furthermore, the Hubble Space Telescope revealed that it has double nucleuses in the core.

In the case of rotating galactic seeds, the galaxy presents spiral arms. We call those with arms as the "**spiral double-disc galaxy**". NGC 5861 is close to Fig. 19(c) with about $\Omega_{1.1} = \pi/8$. NGC 6384 seems close to Fig, 19 (d) with $\Omega_{1.1} = \pi/6$. NGC 3147 is close to Fig. 19(e) with $\Omega_{1.1} = \pi/4$.

Fig. 19. Ring releases from two attached galactic seeds

Rings are released once per $T_{1.1} = 1$ from $T_{1.1} = -24$ to 0: **Double-disc galaxy**

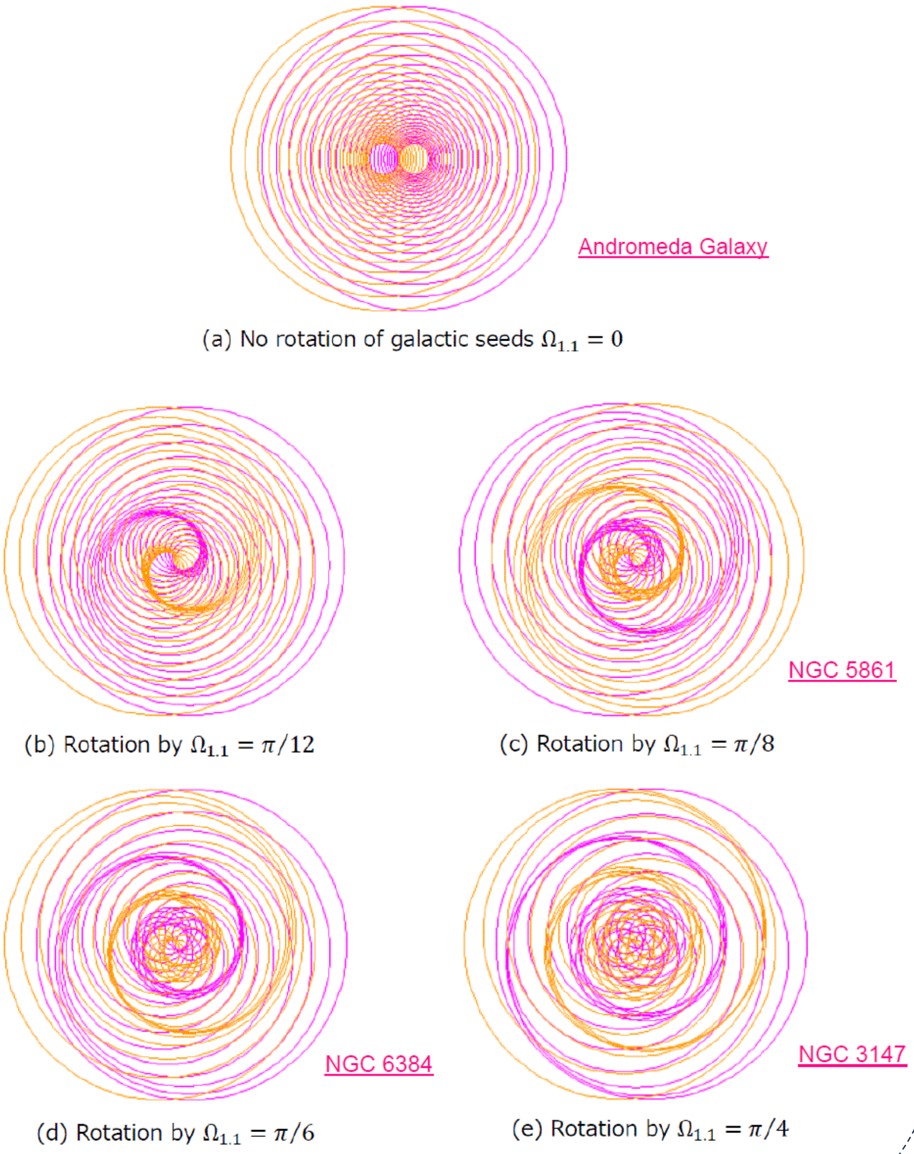

Double-disc galaxy showing spiral arms: **Spiral double-disc galaxy**

The bulge remains over/under each galactic seed by the space expansion if the galactic seeds do not rotate. The two observed nucleuses of the Andromeda Galaxy should be the respective bulges. The reported distance of the two core structures is **4.9 light years**, which should correspond to the **diameter of the galactic seed**.

If the two galactic seeds rotate, the bulges do not follow them but remain at its original location. However, the circulating part of a bulge can no longer keep circulation once separated from the galactic seed, and linearly move away. Only the stationary part remains. Let 0.3 be the initial radius of the bulge, where one is the radius of the galactic seed. By the space expansion, both the location from the center and the radius of the bulge increase. Fig. 20 is the simulation of the current locations of bulges for the galaxy of Fig. 19(c) with $\Omega_{1.1} = \pi/8$, expressed as follows.

Current distributions of bulges in Fig. 20(a):

$$[x_m, y_m]_1 = [r_m \sin t + R_m \cos(m\Omega_{1.1}),\ r_m \cos t + R_m \sin(m\Omega_{1.1})] \quad (101)$$

$$[x_m, y_m]_2 = [r_m \sin t - R_m \cos(m\Omega_{1.1}),\ r_m \cos t - R_m \sin(m\Omega_{1.1})] \quad (102)$$

$$r_m = 0.3 * 1.1^m, \qquad R_m = 1.1^m, \qquad \Omega_{1.1} = \pi/8 \qquad (103)$$

$$m = 0 \text{ to } 24$$

Fig. 20. Bulges of a spiral-double disc galaxy

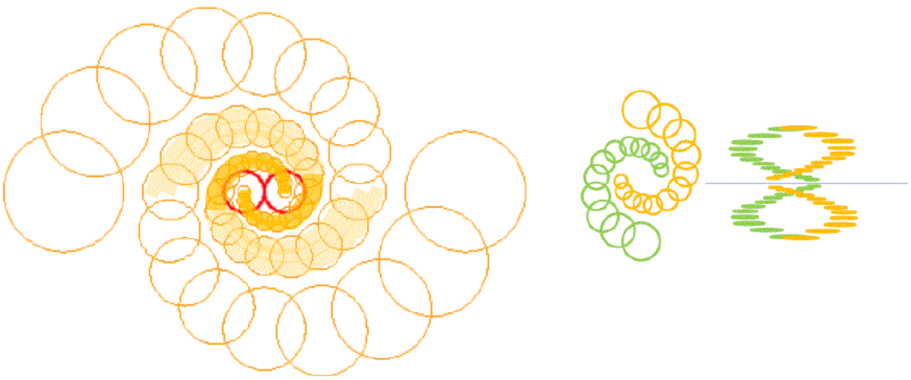

(a) Bulge: $T_{1.1} = -24$ to 0, $\Omega_{1.1} = \pi/8$, $r_{bulge} = 0.3$

The bulges gradually depart from the plane of galactic seeds by the space expansion. While expressed by circles, they are rather continuously distributed.

Fig. 21 is the overlap of Fig. 19(c) of the disc and Fig. 20(a) of the bulges for $\Omega_{1.1} = \pi/8$. As we see in the figure, the bulges are spread between the two major arms. In the case of a spiral double-disc galaxy, it is difficult to detect its bulge because spread widely.

Fig. 21. Overall appearance of a spiral double-disc galaxy

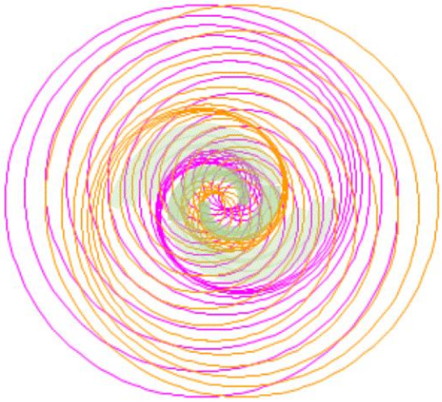

Spiral double-disc galaxy ($T_{1.1} = -24$ to 0, $\Omega_{1.1} = \pi/8$)

(Double-disc + bulge)

✧ Attached then binary galactic seeds – ring releases (Type 3-2)

The radius of a galactic seed gradually decreases by releasing stellar seeds. Two attached galactic seeds keep attached in general even if their radiuses decrease a little. However, if the decrease of energy and the rotating speed are notable, the two galactic seeds turn to separate by the space expansion. In this case, it is possible that rings are released firstly from attached two and then from separate binary galactic seeds. It forms a mixed one of a spiral double-disc galaxy and a barred ring galaxy.

Let us see the following case:

(1) From $T_{1.1} = -24$ to $T_{1.1} = -13$, rings are released from two attached galactic seeds of the radius $r = 1$ with the rotating angular velocity $\Omega_{1.1} = \pi/6$.

(2) From $T_{1.1} = -12$ to $T_{1.1} = 0$, the galactic seed radius is reduced to be $r = 0.5$.

In (2), the rotation radius increases from $R_{12} = 1$ and the rotating angular velocity decreases from $\Omega_{1.1}(-12) = \Omega_{12}$ by the space expansion as follows.

$$R_m = 1.1^{12-m} \tag{104}$$

$$\Omega_m = \Omega_{12}\frac{R_{12}}{R_m} = \frac{\pi}{6}\cdot\frac{1.1^m}{1.1^{12}} \tag{105}$$

The phase of the location of a galactic seed at $T_{1.1} = -12$ is $\theta_{12} = 12\pi/6 = 2\pi = 0$. Respective phases for $m = 12$ to 0 are given as follows.

$$\theta_m = \int_{12}^{m} \Omega_m \, dm = \frac{\pi}{6 * 1.1^{12}} \frac{1.1^m - 1.1^{12}}{\log 1.1} \approx 0.557\pi(1.1^m - 3.138) \tag{106}$$

The galactic seed radius should vary continuously in fact. But we treat it constant as 0.5 for convenience.

Current distributions of released rings in Fig. 22(a):

For $m = 13$ to 24:

$$[x_m, y_m]_1 = [r_m \sin t + \cos(m\Omega_{1.1}),\ r_m \cos t + \sin(m\Omega_{1.1})] \tag{107}$$

$$[x_m, y_m]_2 = [r_m \sin t - \cos(m\Omega_{1.1}),\ r_m \cos t - \sin(m\Omega_{1.1})] \tag{108}$$

$$r_m = 1.1^m, \qquad \Omega_{1.1} = \pi/6, \qquad 0 \le t \le 2\pi \tag{109}$$

For $m = 0$ to 12:

$$[x_m, y_m]_1 = [r_m \sin t + R_0 \cos\theta_m, r_m \cos t + R_0 \sin\theta_m] \tag{110}$$

$$[x_m, y_m]_2 = [r_m \sin t - R_0 \cos\theta_m, r_m \cos t - R_0 \sin\theta_m] \tag{111}$$

$$r_m = 0.5 * 1.1^m, \qquad R_0 = 1.1^{12}, \qquad \theta_m = 0.557\pi(1.1^m - 3.138) \tag{112}$$

Fig. 22(a) is the simulated results.

Fig. 22(b) shows the locations of bulges for the above case. Because the two galactic seeds are rotating, only the stationary part of bulge remains there. We tentatively treat the radius of a bulge be 0.3 times that of the galactic seed. In this case, let $r_0 = 0.3$ be the initial radius for $13 \le m \le 24$ and $r_0 = 0.15$ for $0 \le m \le 12$.

Current distributions of bulges in Fig. 22(b):

For $m = 13$ to 24: $(0 \le t \le 2\pi)$

$$[x_m, y_m]_1 = [r_m \sin t + R_m \cos(m\Omega_{1.1}),\ r_m \cos t + R_m \sin(m\Omega_{1.1})] \quad (113)$$

$$[x_m, y_m]_2 = [r_m \sin t - R_m \cos(m\Omega_{1.1}),\ r_m \cos t - R_m \sin(m\Omega_{1.1})] \quad (114)$$

$$r_m = 0.3 * 1.1^m, \qquad R_m = 1.1^m, \qquad \Omega_{1.1} = \pi/6 \qquad (115)$$

For $m = 0$ to 12: $(0 \le t \le 2\pi)$

$$[x_m, y_m]_1 = [r_m \sin t + R_0 \cos\theta_m,\ r_m \cos t + R_0 \sin\theta_m] \quad (116)$$

$$[x_m, y_m]_2 = [r_m \sin t - R_0 \cos\theta_m,\ r_m \cos t - R_0 \sin\theta_m] \quad (117)$$

$$r_m = 0.15 * 1.1^m, \qquad R_0 = 1.1^{12}, \qquad \theta_m = 0.557\pi(1.1^m - 3.138) \qquad (118)$$

The intensity of bulges is too much diluted in $13 \le m \le 24$. We may account only $0 \le m \le 12$ for bulges.

Fig. 22(c) shows the overall appearance of the resulted galaxy including the disc (double-disc and rings), bulge and bar-bulge. We call this type of galaxies as the "**barred ring & double-disc galaxy**" (Type 3-2). NGC 105 is an example of this type. If the timing of separation of two attached galactic seeds is earlier, it results in almost a barred ring galaxy with fringe, an example of which is NGC 7329.[20]

Fig. 22. Ring releases from rotating two attached then binary galactic seeds

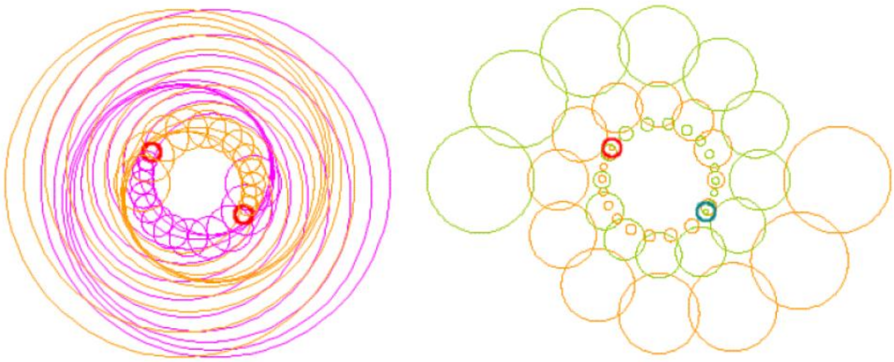

(a) Disc by ring releases (b) Bulge by orthogonal releases

(1) $T_{1.1} = -24 \text{ to } -13:\ r = 1,\ R = 1,\ r_{bulge} = 0.3,\ \Omega_{1.1} = \pi/6$

(2) $T_{1.1} = -12 \text{ to } 0:\ \ r = 0.5,\ R_m = 1.1^m,\ R_0 = 1.1^{12} = 3.14,\ r_{bulge} = 0.15,$

$\theta_m = 0.557\pi(1.1^m - 3.138)$

Overall appearance of the galaxy (double-disc & ring + bulge + bar-bulge)

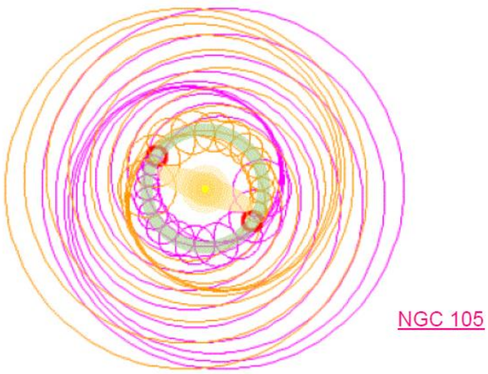

(c) Barred ring & double-disc galaxy

As explained in this chapter, the ECT has successfully demonstrated the formation of various types of galaxies by simulation. It is a big contrast to the standard physics, which cannot demonstrate anyone except for elliptical galaxies even if they tried to explain by introducing a massive black hole at the center ant dark matter in the halo.

Chapter 7: Elementary single circulations and light

7.1. Elementary single energy circulations

✧ Elementary single circulation

As the space expands, a stellar seed further releases daughter circulations, and finally causes a cyclic decomposition to form a proto-stellar system with a star in the center.

The smallest one of the energy circulations released in this way is the "**elementary single circulation**" that has the same radius μ_0 as that of the spacia. As an energy circulation quantized in the 4D space, any one of a smaller radius than it is impossible. We express an elementary single circulation in **hidden-space dimensions** as iS, and that in **space-space dimensions** as S. The elementary single circulation has the same circulating velocity as that of the spacia shown by Eq. (47), and let m_0 be its intrinsic energy. Its energy distribution and amount are shown as follows.

$$E_{(iS)}\psi_{iS} = E_{(iS)}[X \quad H] = E_{(iS)}\mu_0(\cos\omega_0 t + i\sin\omega_0 t) \tag{119}$$

$$E_{(S)}\psi_S = E_{(S)}[X \quad Y] = E_{(S)}\mu_0(\cos\omega_0 t + j\sin\omega_0 t) \tag{120}$$

$$E_{(iS)} = E_{(S)} = m_0 {v_c}^2 = m_0 {\mu_0}^2 {\omega_0}^2 \tag{121}$$

We call the coupled conjugate pair consisting of two conjugate circulations as the "**double circulation**" shown by iD or D. The circulating velocity of the double circulation is $v_c = \pm\mu_0\omega_0$. What is quantized within a spacia is defined as the "**quantum particle**". A quantum particle has the radius μ_0, and is a composition of single and/or double circulations, and/or their excited form within a spacia.

7.2. Definition of electric charge and electric force

✧ Definitions of the electric charge and the magnetic charge

As shown in Eq. (2), the charge of the fundamental force is a momentum, which is a vector having a direction. The direction in the hidden dimension H is orthogonal to any directions in the three space dimensions. Therefore, the angular factors in Eq. (2) disappear for the force in a space direction between two momentums in H. Since H is one dimension, a momentum there and the distance direction are on one plane. If we take $\cos\theta_p = 1$, θ_1 and θ_2 are $+\pi/2$ or $-\pi/2$, and $\sin\theta_1$, $\sin\theta_2 = +1$ or -1. Therefore, the charge for this force is a scalar, and take a plus or minus value. In the ECT, the momentum in the hidden dimension H of a hidden-space dimensional circulation is defined as the "**electric charge**". The electric charge takes a plus or minus value depending on the direction of momentum in H. In addition, the momentum in the space dimensions of a hidden-space circulation is defined as the "**magnetic charge**". In the 3D space, the electric charge is a **scalar charge** but the magnetic charge is a **vector charge**.

✧ Electric force

Let us examine the intra-circulation force of iS; the hidden-space single circulation. The force between two local momentums on the circumference was shown by Eq. (17). In order to find the component in the space direction X of the intra-circulation force of iS, we divide the circulation into two halves of the angles α and β as shown below.

$$-\frac{\pi}{2} \leq \alpha \leq \frac{\pi}{2}\,, \qquad \frac{\pi}{2} \leq \beta \leq \frac{3\pi}{2}\,, \qquad \theta \equiv \beta - \alpha \tag{122}$$

The force between $\mathbf{\Delta p_\alpha}$ and $\mathbf{\Delta p_\beta}$ becomes as below from Eq. (17).

$$\Delta F = K_f \frac{\Delta p_\alpha \Delta p_\beta}{d^2} \sin\frac{\theta}{2} \sin\frac{-\theta}{2} = -K_f \frac{\Delta p_\alpha \Delta p_\beta}{4{\mu_0}^2} \tag{123}$$

The component in the space direction is

$$\Delta F_x = \Delta F \cos\gamma = \Delta F \sin\frac{\alpha+\beta}{2} = \Delta F\left(\sin\frac{\alpha}{2}\cos\frac{\beta}{2} + \cos\frac{\alpha}{2}\sin\frac{\beta}{2}\right). \tag{124}$$

γ is the angle #6 in Fig. 23, and given by

$$\gamma = \frac{\pi}{2} - \frac{\theta}{2} - \alpha = \frac{\pi}{2} - \frac{\alpha+\beta}{2}. \tag{125}$$

Fig. 23. Local momentums of an energy circulation and their

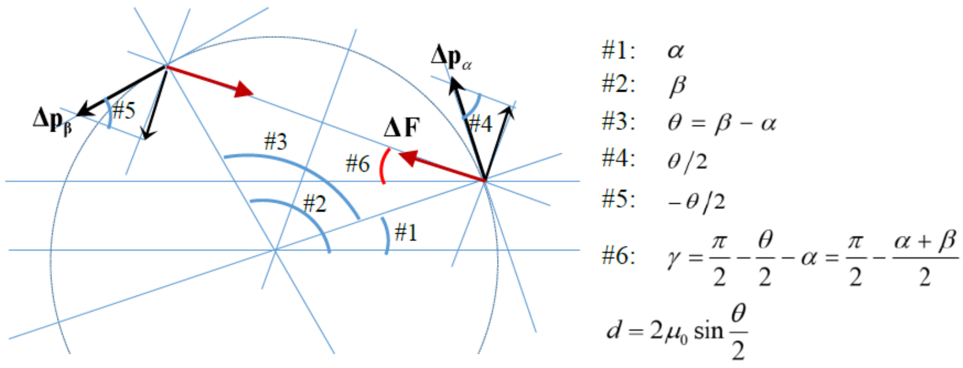

The component in the X direction of the force that $\Delta\mathbf{p}_\alpha$ receives from the entire momentum $\mathbf{p}_\pi$ in the half circle arc $\frac{\pi}{2} \le \beta \le \frac{3\pi}{2}$ gets as follows.

$$p_h \equiv p_\pi = \Delta p_\beta \int_{\pi/2}^{3\pi/2} d\beta = \Delta p_\beta \pi, \qquad \Delta p_\beta = p_h/\pi \tag{126}$$

$$\begin{aligned} F_x(\alpha) &= \int_{\pi/2}^{3\pi/2} \Delta F_x \partial\beta = \int_{\pi/2}^{3\pi/2} \Delta F\left(\sin\frac{\alpha}{2}\cos\frac{\beta}{2} + \cos\frac{\alpha}{2}\sin\frac{\beta}{2}\right)\partial\beta \\ &= -K_f \frac{\Delta p_\alpha}{4{\mu_0}^2}\frac{p_h}{\pi} 2\sqrt{2}\cos\frac{\alpha}{2} \end{aligned} \tag{127}$$

The component in X of the force that the momentum $\mathbf{p}_0$ of the half circle arc $-\frac{\pi}{2} \le \alpha \le \frac{\pi}{2}$ receives from the momentum $\mathbf{p}_\pi$ of the other half-circle arc $\frac{\pi}{2} \le \beta \le \frac{3\pi}{2}$ is given as below.

$$\begin{aligned} F_x &= \int_{-\pi/2}^{\pi/2} F_x(\alpha)\partial\alpha = -K_f \frac{2\sqrt{2}}{4{\mu_0}^2}\frac{{p_h}^2}{\pi^2}\int_{-\pi/2}^{\pi/2}\cos\frac{\alpha}{2}\partial\alpha \\ &= -\frac{8}{\pi^2}K_f\frac{{p_h}^2}{(2\mu_0)^2} \end{aligned} \tag{128}$$

This is the intra-circulation force of iS in the space direction.

Here, we define the half circle momentum p_h as the "**elementary electric charge**" e and the constant K_e as follows.

$$K_e \equiv \frac{8}{\pi^2} K_f \,, \qquad e \equiv p_h = \frac{m_0 \mu_0 \omega_0}{2} = \frac{m_0 c}{2} \tag{129}$$

If we express the intra-circulation force of Eq. (128) by the electric charge, it becomes as follows.

$$F_x = -\frac{8}{\pi^2} K_f \frac{{p_h}^2}{(2\mu_0)^2} = -K_e \frac{e^2}{(2\mu_0)^2} \tag{130}$$

This is the "**electric force**" that acts in the **space direction** between the electric charges in an iS.

7.3. Elementary charge pair eCP

✧ Elementary charge pair

When an iS absorbs a light (light quantum) and energy is added, it prolongs in the space dimension to plural (n) circulations over n spacias as shown in Fig. 11. The number n of circulations is limited to an odd number. This prolonged one is called as the "**elementary charge pair** (**eCP**)".

Fig. 24. Prolongation of hidden-space single circulation iS

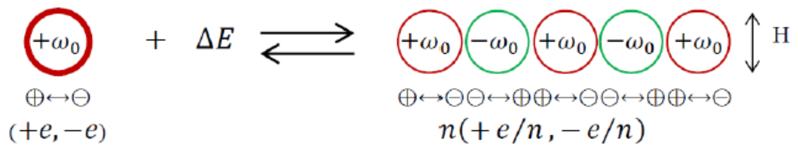

Electric charge = momentum in the hidden dimension H

✧ Connected electric force

By the addition of energy, the potential energy in the space direction is increased, but the sum of the momentums in the hidden dimension, that is, that of electric charges does not change. The space directional force in each circulation is given as follows from Eq. (130).

$$F_x = K_e \frac{(e/n)(-e/n)}{(2\mu_0)^2} = -K_e \frac{e^2}{(2n\mu_0)^2} = -K_e \frac{e^2}{d^2} \qquad (131)$$

At each adjacent part of two circulations, the outward and inward intra-circulation forces set off each other to be zero. The force of Eq. (131) remains only at the two ends of an elementary charge pair. This is equal to the virtual force if it is assumed that elementary charges $+e$ and $-e$ would be separated by the distance $d = n \times 2\mu_0$ (length of eCP). This is the true feature of the electric force acting between an electron and a proton. The electric charges $+e$ and $-e$ are dispersed between the proton and electron, and each of the elementary charge is the sum of the charges. In an atom, the electron-proton pair includes an eCP. In an electron, a neutrino is attached to the minus end of an eCP, and in a proton, a space-space single circulation is attached to the plus end of an eCP (proton includes also other circulations). We named this force within an eCP as the "**connected electric force**". Thus, the force between a proton and an electron is a connected electric force, not an electrostatic force between isolated electric charges.

✧ Energy of an elementary charge pair (polarization energy)

The length of an eCP changes by absorption or emission of light (light quantum).

$$eCP(x) + \gamma \rightleftarrows eCP(x + \Delta x)\,, \qquad x = 2n\mu_0 \qquad (132)$$

The smallest eCP is iS of $n = 1$. If we express the energy of eCP as

$$E_{(n-iS)} = m_0 c^2 + \Delta E\,, \qquad (133)$$

ΔE is the increase in electric potential energy from iS. Here, as the potential energy at $x = 2\mu_0$ we set the energy of iS.

$$U(2\mu_0) \equiv E_{(iS)} = m_0 c^2 \tag{134}$$

$$\Delta E = U(x) - U(2\mu_0) = \int_{2\mu_0}^{x} (-F_x) dx = \int_{2\mu_0}^{x} K_e \frac{e^2}{x^2} dx \tag{135}$$

Then, the electric potential energy of an eCP becomes equal to the total energy of the eCP.

$$U(x) = \Delta E + U(2\mu_0) = K_e e^2 \left(\frac{1}{2\mu_0} - \frac{1}{x} \right) + m_0 c^2 \quad (x \geq 2\mu_0) \tag{136}$$

We call this energy of eCP as the "**polarization energy**".

If an eCP is prolonged by addition of energy to $U(x)$, the added energy is expressed as below.

$$\Delta E = U(x + \Delta x) - U(x) = K_e e^2 \left(\frac{1}{x} - \frac{1}{x + \Delta x} \right), \qquad \Delta E_{max} = \frac{K_e e^2}{x} \tag{137}$$

The energy addition is made by absorbing one cycle of light (light quantum), but the added energy will remain within the eCP. Therefore, the increase in energy (per one second) is $\Delta E = h\nu^2$. Conversely, when an eCP becomes shorter, the difference energy is released as light. In this case, the light emission is that of a light quantum of one cycle, and is not a continuous light. Regarding the light, we will explain in detail in the next section.

The added energy ΔE has a maximum. If an eCP absorbs a light of higher energy than the maximum (**higher frequency**), it will **divide to two**.

$$eCP(x) + \Delta E \longrightarrow eCP(x_1) + eCP(x_2) \tag{138}$$

✧ Magnetic rotation

The magnetic charge of a static eCP is zero since those of opposite directions are set off. An eCP can rotate around the hidden dimension axis, and its velocity components in each space direction can flexibly change. By rotating around the H axis, a free eCP with nothing added to either end is rotating in the space dimensions around its center. It shows the "**rotating magnetic charge**", which is the core feature of the magnetism.

7.4. Rotation of iS and light radiation

✧ **Rotation of iS around the hidden dimension axis H**

There are three planes orthogonal to each other in 3D, but are six planes in 4D; XY, YZ, ZX, HX, HY, HZ. When an iS rotates around the hidden dimension axis H, it rotates in space dimensions, but there is no variation in H. Therefore, no energy is lost by the light radiation. By a rotation around the H axis, the circulating velocity in the space dimension of iS can be flexibly divided to each space components.

$$v_x{}^2 = c^2 \implies v_x{}^2 + v_y{}^2 + v_z{}^2 = c^2 \tag{139}$$

✧ **Light radiation by rotation of iS around a space axis**

If we make an iS rotate around a space dimension axis, it will emit the light because it cannot rotate to a mixed direction of hidden and space dimensions. Let us take a look at the details below. First, consider an iS in X-H.

$$E_{(iS)}[X \quad H] = m_0 \mu_0{}^2 \omega_0{}^2 \, \mu_0(\cos\omega_0 t + i\sin\omega_0 t) \tag{140}$$

Add an energy ΔE and make iS rotate around a space axis Z by $\omega < \omega_0$.

$$\Delta E = m_0 \mu_0{}^2 \omega^2 \tag{141}$$

In addition to the circulation by Eq. (140), the following circulation shall be tried to be added to the intrinsic energy m_0.

$$[\mathrm{X} \quad \mathrm{H}] = \mu_0(\cos\omega t + i\sin\omega t)\,, \qquad [\mathrm{X} \quad \mathrm{Y}] = \mu_0(\cos\omega t + j\sin\omega t) \tag{142}$$

However, in order to be quantized as a particle, its frequency should be an integral multiple of ω_0. Therefore, the additional energy cannot rotate and will move linearly in the space direction X while vibrating. The vibrations in

H and Y propagate in two directions; +X and -X, this is the "**light radiation**". The energy of the light radiation to one direction is as follows.

$$E_\gamma = \frac{\Delta E}{2} = \frac{m_0 {\mu_0}^2}{2}\omega^2 \ \text{(energy of light)}\,. \tag{143}$$

The propagation speed in the X direction is the circulating velocity of the spacia, which is the light speed.

$$v_x = \mu_0 \omega_0 = c \tag{144}$$

✧ **Energy position of radiated light**

The energy of the additional circulation shown by Eqs. (141) and (142) is radiated in the X direction, and does not remain on the circumference of iS. However, this rotation is applied continuously from the outside, and Eq. (141) shows the energy per one second. We can regard that the energy is continuously supplied and light is emitted to two directions; -X at the phase of $\theta = 0$ of the circulation of Eq. (142) and +X at that of $\theta = \pi$.

Since the propagation velocity is Eq. (144), the wavelength is expanded from the circumference of $2\pi\mu_0$ by ω_0/ω times, and given by the below formula, in which $\nu = \omega/2\pi$ is the frequency of the light.

$$\lambda = 2\pi\mu_0 \frac{\omega_0}{\omega} = \frac{\mu_0\omega_0}{\nu} = \frac{c}{\nu} \tag{145}$$

Here, let us see the energy position of the radiated light from the phase of $\theta = 0$. As shown in Fig. 25, the position of the light in X is given by the following formula.

$$\mathbf{X} = (-\mu_0\omega_0 t + \mu_0)\mathbf{e_x} \ \ (\approx -\mu_0\omega_0 t\mathbf{e_x} = -ct\mathbf{e_x}) \tag{146}$$

The second term, μ_0, can be ignored except for immediately after the radiation. The position in H is given as follows.

$$\mathbf{H} = \mu_0 \sin\omega t\, \mathbf{e_h} \tag{147}$$

The position in Y is given by the following formula because the rotation velocity of $\mu_0\omega$ propagates to surrounding spacias at the speed of $\mu_0\omega_0$, so that the amplitude becomes larger. (similar to Eq. (145) for wavelength)

$$\mathbf{Y} = \frac{\omega_0}{\omega}\mu_0 \sin\omega t\, \mathbf{e_y} \tag{148}$$

In Fig. 25, we show the energy locations of the radiated lights from $\theta = 0$ and $\theta = \pi$.

Fig.25. Energy locations of radiated lights by rotating *iS* (hidden-space single circulation) around the Z axis

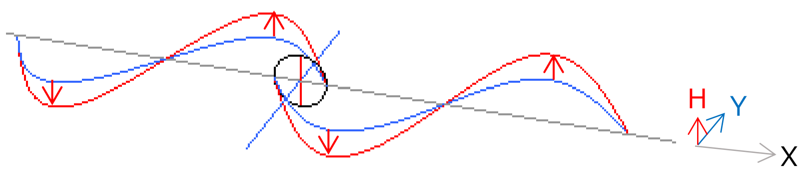

Red; 4D expression Blue: 3D expression $Z = 0$ (not expressed)

✧ Vibrations of electric and magnetic charges of radiated light

The velocities in H and Y are as follows.

$$\mathbf{v_h} = \frac{d\mathbf{H}}{dt} = \omega\mu_0 \cos\omega t\, \mathbf{e_h} \tag{149}$$

$$\mathbf{v_y} = \frac{d\mathbf{Y}}{dt} = \omega_0\mu_0 \cos\omega t\, \mathbf{e_y} \tag{150}$$

The half circle momentum in the case that the energy of Eq. (141) circulates by Eq. (142) is the **electric charge** and the **magnetic charge**. Since the vibration parts other than the amplitude as well as the direction are equal to those of the velocity, the momentums are shown as follows.

$$e_\gamma = b_\gamma = p_h = \frac{m_0\mu_0}{2}\omega \tag{151}$$

$$\mathbf{e_\gamma} = e_\gamma \cos\omega t\, \mathbf{e_h} \tag{152}$$

$$\mathbf{b_\gamma} = b_\gamma \cos\omega t\, \mathbf{e_y} \tag{153}$$

If the electric charge and magnetic charge in Eqs. (152) and (153) are expressed in sine like the location in Y, they are as below.

$$\mathbf{e_\gamma} = \frac{m_0\mu_0}{2}\sin(\omega t + \pi/2)\, \mathbf{e_h}\,, \qquad \mathbf{b_\gamma} = \frac{m_0\mu_0}{2}\sin(\omega t + \pi/2)\, \mathbf{e_y} \tag{154}$$

We can see that the vibrations in electric and magnetic charges are advanced by $\pi/2$ than the energy location in Y.

✧ Representation of light propagation as a plane wave

If we express the propagation to X of electric charge as a plane wave in the X-H plane and that of magnetic charge and that of the position in Y as plane waves in the X-Y plane, they become as follows. k is the wave number (angular wave number) given by $k = \omega/c$.

$$\mathbf{e_\gamma} = \frac{m_0\mu_0}{2}\omega\cos(kx - \omega t)\,\mathbf{e_h} = \frac{m_0\mu_0}{2}\omega\sin\big(kx - (\omega t + \pi/2)\big)\,\mathbf{e_h} \qquad (155)$$

$$\mathbf{b_\gamma} = \frac{m_0\mu_0}{2}\omega\cos(kx - \omega t)\,\mathbf{e_y} = \frac{m_0\mu_0}{2}\omega\sin\big(kx - (\omega t + \pi/2)\big)\,\mathbf{e_y} \qquad (156)$$

$$\mathbf{Y} = \frac{\omega_0}{\omega}\mu_0\sin(kx - \omega t)\,\mathbf{e_y} \qquad (157)$$

✧ Bremsstrahlung (braking radiation)

What have been explained above is for the case that an iS is stationary at $(x, y) = (0,0)$. However, in reality, the rotation around the Z axis is given by making an iS or eCP orbit with a radius $r \neq 0$. If we adopt an X-Y coordinate system that rotates around $y = -r$ with the light radiation direction as the X-axis and the radial direction as the Y-axis, the position of iS is always $(x, y) = (0,0)$, so that the all equations about the light emission, which have been shown above so far, are applied as they are. The light radiation direction X is the tangential direction of each point on the orbit. This type of **light radiation** is called as the "**bremsstrahlung**" (or braking radiation), and emits continuous light. There is another type of **light emission** that an energy difference is released as light when an eCP gets shorter.

✧ Energy of light quantum and the Planck constant

The energy of light is given by Eq. (143), which shows a value for one second. Here, we define the one cycle of light as the "**light quantum**".

The light quantum is same as so called the photon, but is not a particle. The energy of a light quantum (photon) is given by the following formula.

$$E_q \equiv \frac{E_\gamma}{\nu} = \frac{2\pi}{\omega}\frac{m_0{\mu_0}^2}{2}\omega^2 = \pi m_0{\mu_0}^2\omega$$
$$= 2\pi^2 m_0{\mu_0}^2\nu \quad \text{(energy of light quantum)} \tag{158}$$

Here, the **Planck constant** h has been given by m_0 and μ_0.

$$h = 2\pi^2 m_0{\mu_0}^2 \ \text{(Planck constant)} \tag{159}$$

As shown here, the Planck constant is invariant by the space expansion, but is obtained by m_0 and μ_0. Using the Planck constant, the energies of light and light quantum (photon) are shown by the following formulas, which do not change as the space expands.

$$E_\gamma = h\nu^2\,, \qquad E_q = h\nu \tag{160}$$

Cautions about energy quantum (light quantum) and energy

- **Energy** is an amount conserved over time and is expressed as a value **per unit time (one second)**. (All the speed, momentum, and frequency in the formulas written so far are values per one second. The energy described by them is also an amount per second.)
- The energy quantum including light quantum is defined as the energy per one cycle $E_q \equiv E/\nu$. This is an energy amount per $1/\nu$ second.
- When an energy circulation absorbs one cycle of light quantum $E_q = h\nu$, the added energy remains on its circumference. Therefore, the increase in energy (per second) of it is $\Delta E = h\nu^2$.
- When a light quantum (e.g. gamma ray) is moving linearly, its energy per one second is $E = h\nu^2$, but its position moves a distance of light speed times one second. In this case, the energy passing through one point is $E_q = h\nu$, and the passing time is $1/\nu$ second.
- The energy of continuous light passing at a point per second is $E = h\nu^2$.

Conclusion: The energy of light is $E = h\nu^2$.

✧ Light speed variation by the space expansion

An elementary single circulation is given by doubling the circulating velocity of one of the two conjugate circulations in a spacia. Therefore, it has the same radius μ_0 and circular frequency ω_0 as those of the spacia. If the frequency of an energy is an integral multiple of ω_0, it becomes a quantized circulation (particle), but if it is smaller than ω_0, it is not quantized and propagates linearly in the space energy. This kind of radiation in hidden-space dimensions is the **light**, the propagation speed of which is the circulating velocity of the spacia.

$$c = v_c = \mu_0 \omega_0 \tag{161}$$

As the space expands, the number of spacias increases, but at this time, the radius μ_0 of the spacia remains unchanged, and the frequency ω_0 decreases. The light speed c also decreases as ω_0 decreases. When the cosmic radius becomes x from x_0, the number of spacias increases to the cube of x/x_0. The intrinsic energy m_μ of the spacia is invariant, and the total energy does not change, either. When ω_0 is expressed as a function of the cosmic radius x, we have the following relation.

$$m_\mu {\mu_0}^2 \big(\omega_0(x_0)\big)^2 = \frac{x^3}{{x_0}^3} m_\mu {\mu_0}^2 \big(\omega_0(x)\big)^2 \tag{162}$$

If we express the light speed as a function $c(x)$ of the radius, we get the below formula.

$$c(x) = \sqrt{\frac{{x_0}^3}{x^3}} * c(x_0) \tag{163}$$

Since ${x_0}^3/x^3$ is equal to the ratio of the space energy density, this Eq. (163) indicates that the light speed is proportional to the square root of the medium density. As the space expands, the energy of the elementary single circulation shown by Eq. (121) also decreases as ω_0 decreases (the intrinsic energy m_0 remains constant). However, the following relation of it to the light speed remains unchanged.

$$E_{(iS)} = E_{(S)} = m_0 c^2 \tag{164}$$

In the Section 8.2 of the next chapter, we will derive the light speed equation based on another time; per the change of the cosmic radius.

Chapter 8: Hubble diagram

8.1. Speed of the space expansion

✧ Motion of the whole universe

The motion of the whole cosmic energy, which is the sum of the space energy and the apparent energy, can be expressed by Eq. (41) in 4D and by Eq. (45) in 3D provided that the radius μ is increasing. Let us see the expanding speed of the cosmic radius.

Let M_U be the intrinsic energy of the whole universe circulating at the velocity V_c. We take the local intrinsic energy in the local area of unit angles.

$$M_U \equiv E_U/{V_c}^2 \,, \qquad m_\theta \equiv \Delta E_\theta/{V_c}^2 \qquad (165)$$

In the radial direction x, the change in the kinetic energy and that of the potential energy are set off each other. Therefore, the intrinsic energy m_θ for the circulation is invariant by x. Because ΔE_θ is also invariant, **V_c is constant** as the space expands. All of $E_U, M_U, \Delta E_\theta, m_\theta$ and V_c are invariant by x.

✧ Acceleration and velocity of the expansion of cosmic radius

From Eq. (18) for the intra-circulation force, the force on a local intrinsic energy ΔE_θ is given as follows, where $p = E_U/V_c$.

$$F_x = -K_f \frac{p_U \Delta p_\theta}{2\pi x^2} = -K_f E_U \frac{m_\theta}{2\pi x^2} \qquad (165)$$

K_f here is not for the light speed, but for V_c. Because the motion of the space expansion is without a medium, it obeys the Newtonian equation of motion.

$$F_x = m_\theta \alpha \qquad (166)$$

Therefore, the acceleration of the radius is given as follows from Eq. (165).

$$\alpha = \frac{dV_x}{dt} = -K_f E_U \frac{1}{2\pi x^2} \tag{167}$$

Integrate the both sides by x from $x_0(V_x = V_0)$ to $x(V_x = V_x)$.

$$\int_{x_0}^{x} \frac{dV_x}{dt} dx = \int_{V_0}^{V_x} V_x dV_x = -\frac{K_f E_U}{2\pi} \int_{x_0}^{x} \frac{1}{x^2} dx \tag{168}$$

$$\frac{1}{2}\left({V_x}^2 - {V_0}^2\right) = \frac{K_f E_U}{2\pi}\left(\frac{1}{x} - \frac{1}{x_0}\right) \tag{169}$$

$${V_x}^2 = \frac{K_f E_U}{\pi}\left(\frac{1}{x} - \frac{1}{x_0} + \frac{\pi {V_0}^2}{K_f E_U}\right) \equiv \frac{K_f E_U}{\pi}\left(\frac{1}{x} - K\right) \tag{170}$$

$$V_x = \pm\sqrt{\frac{K_f E_U}{\pi}\left(\frac{1}{x} - K\right)} \tag{171}$$

The radius x has the maximum at $V_x = 0$. Let us define and use the "**cosmic unit**" of length, in which $x = 1$ at $V_x = 0$. Then, $K = 1$ in Ex. (171). The **expansion speed of cosmic radius** is given as below by the cosmic unit.

$$V_x = \pm\sqrt{\frac{K_f E_U}{\pi}\left(\frac{1}{x} - 1\right)} \tag{172}$$

After x reaches zero, it will turn to decrease, that it, to shrink.

8.2. Light speed variation by the space expansion

✧ Light speed per variation of the cosmic radius

The light speed as a function of the radius was given by Eq. (163). Rewrite the constant part as K_1.

$$c(x) = \sqrt{\frac{{x_0}^3}{x^3}} * c(x_0) \equiv \frac{K_1}{\sqrt{x^3}} \tag{173}$$

The cosmic radius can be used as an alternative time, by which other movements are traced. We named it as the "**Observed Time**", and the usual time as the "**original time**". Let us derive the light speed per Observed Time $C(x)$. If you feel uncomfortable with the Observed Time, please just take it as the light speed per variation of the cosmic radius.

$$C(x) \equiv \frac{dLD}{dx} = \frac{dLD}{dt}\frac{dt}{dx} = c(x)\frac{1}{V_x} \tag{174}$$

From Eqs. (172) (173), $C(x)$ is given as follows.

$$C(x) = \pm \frac{K_1}{\sqrt{\frac{K_f E_U}{\pi} x^3 \left(\frac{1}{x} - 1\right)}} \tag{175}$$

Rewrite the constant part as K, then we get the light speed per variation of x as follows.

$$C(x) = \pm \frac{K}{x\sqrt{(1-x)}} \quad (T_c \leq x < 1) \tag{176}$$

In very small values of x, the apparent light speed slows down due to scattering. We call the factor as the **electromagnetic factor** f_{EM}. The factor of Eq. (176) as the **density factor** f_d. Strictly saying, $C(x)$ is given as below.

$$C(x) = K * f_d * f_{EM} = \pm K \frac{1}{x\sqrt{(1-x)}} \left(1 - \frac{{T_c}^3}{x^3}\right) \tag{177}$$

T_c is the "Time to clear", which is the Time (or radius) when the space became transparent to light. We do not know the value, but expect it as between 10^{-5} and 10^{-3}. The graph of Eq. (177) is given in Fig. 26.

Fig.26. Light speed per variation of the cosmic radius

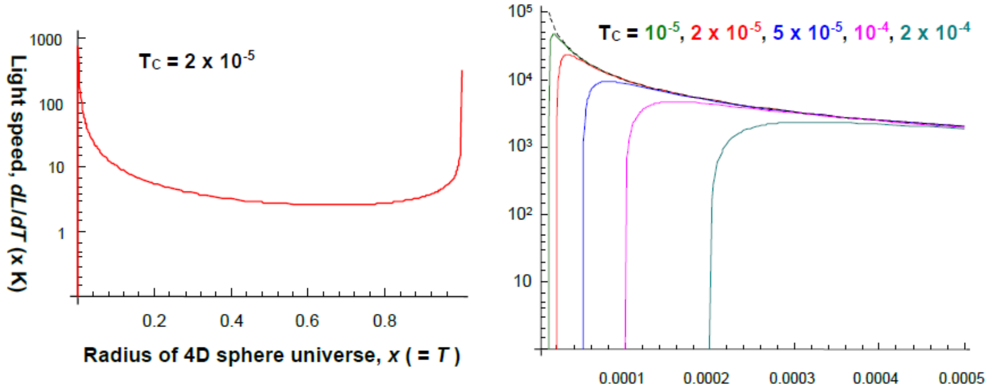

Time-course of light speed by the Observed Time (semi logarithmic scale)

8.3. Redshift

The **redshift** here means the prolongation of wavelength by the space expansion, defined as follows.

$$z \equiv n - 1 \tag{178}$$

Since the light was emitted, the space has been expanded by n times. In actual observation, we cannot detect the original wavelength at the emission, so compare with the present wavelength of the same element. Let us confirm the relation of Eq. (178).

The energy of light is given by $E_\gamma = h\nu_{(x)}{}^2$ and proportional to $m_0 C_{(x)}{}^2$. Therefore, the frequency $\nu_{(x)}$ is proportional to the light speed $C_{(x)}$. We treat the radius x as Time, and express as T_E for at emission and as T_p for present. There is the following relation.

$$\frac{\nu_0(T_P)}{\nu_0(T_E)} = \frac{C(T_P)}{C(T_E)} \tag{179}$$

The redshift Z_p by the comparison in wavelength with the present element is given as follows.

$$z_p + 1 = \frac{\lambda(T_P)}{\lambda_0(T_P)} = \frac{\lambda(T_P)}{\lambda_0(T_E)} \times \frac{\lambda_0(T_E)}{\lambda_0(T_P)} = n \times \frac{C(T_E)}{\nu_0(T_E)} \frac{\nu_0(T_P)}{C(T_P)} = n \qquad (180)$$

Thus, we have confirmed that z_p is equal to z.

The redshift is decided only by the space expansion rate, which corresponds to the time and the distance from the emission. As for each celestial body, its Doppler effect is added depending on its speed to the space energy. However, if we measure many stars of the same value of n and take the mean, the Doppler effect can be ignored.

8.4. Distance of stars

There are several types of star distances; the distance when the light was emitted at the star, the current distance when the light reached us now, and the distance for which the light has actually traveled from the star to us.

Fig.27. Light propagation and space expansion

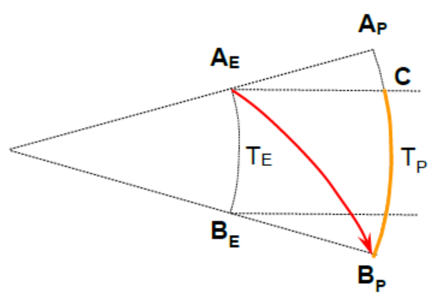

Let us consider the case of Fig. 27. The radius indicates the spherical radius in the 4D space, and the arc shows the distance in the 3D space. The cosmic radius can be treated as time, and is expressed as T here, but if you feel uncomfortable, read it as the cosmic radius x. Consider the case that light is emitted at the location A at time T_E, and arrives at the location B

(Earth) at time T_P (current). The distance at the emission is A$_E$-B$_E$, let D_0 be for which. The light propagates from A$_E$ to B$_P$, but the propagation distance in the 3D space is C-B$_P$. We call it as the "**light propagated distance**" and let LD be for it. The current distance when we observe the light is A$_P$-B$_P$, called as the "**present distance**", let PD be for it. If the space expands by n times, PD will be n times D_0, and LD will be $(n+1)/2$ times D_0 as shown by the following equations.

$$PD = nD_0 \tag{181}$$

$$LD = D_0 + \frac{PD - D_0}{2} = \frac{n+1}{2} D_0 \tag{182}$$

The light propagated distance LD is determined from the observed brightness, and the present distance PD is obtained from the following relation.

$$PD = \frac{2n}{n+1} LD = \frac{2(z+1)}{z+2} LD \tag{183}$$

✧ Light propagated distance LD and its distance modulus

The observed brightness shows the distance information after emission. What is directly measured is the flux, which is the luminosity (= energy per unit time) per unit area. The flux of light, which was emitted at T_E and reaches us at present T_p, is given as follows, in which L is the luminosity and LD is the light propagate distance (or luminosity distance in the standard physics).

$$F(T_E) = \frac{L}{4\pi \cdot LD(T_E)^2} \tag{184}$$

We define the logarithmic magnitude $m(T_E)$ of the flux as follows.

$$m(T_E) \equiv -2.5 \cdot \lg F(T_E) \tag{185}$$

Here, we take the magnitude relative to the same luminosity with $z = 0.05$ on a base-10 logarithmic scale. This is a distance modulus, called as the “**magnitude of LD to z=0.05**”. Let us express it using T_{ER}, which is the relative Time of emission to the present Time T_p, instead of T_E as a variable.

$$T_{ER} \equiv T_E/T_p \tag{186}$$

$z = 0.05$ corresponds to $T_{ER} = 1/1.05$. The distance modulus is defined as

$$DM_{0.05}(T_{ER}) \equiv m(T_{ER}) - m(z = 0.05) = m(T_{ER}) - m(1/1.05)\,. \tag{187}$$

From Eqs. (184), (185) and (186), Eq. (187) becomes as follows.

$$DM_{0.05}(T_{ER}) = 5\mathrm{lg}LD(T_{ER}) - 5\mathrm{lg}LD(1/1.05) \tag{188}$$

The light propagated distance $LD(T_E)$ is obtained by integrating the light speed $C(x)$ by the radius x from T_E to T_p. For the light speed, we can ignore the electromagnetic factor f_{EM} at least when $z < 12.8$. From Eq. (176), $LD(T_E)$ is given as follows.

$$\begin{aligned} LD(T_E) &= \int_{T_E}^{T_p} C(x)dx = \int_{T_E}^{T_p} \frac{K}{x\sqrt{1-x}}dx = K\left(\log\frac{1-\sqrt{1-T_p}}{1+\sqrt{1-T_p}} - \log\frac{1-\sqrt{1-T_E}}{1+\sqrt{1-T_E}}\right) \\ &= K\log\left(\frac{1-\sqrt{1-T_p}}{1+\sqrt{1-T_p}}\cdot\frac{1+\sqrt{1-T_E}}{1-\sqrt{1-T_E}}\right) \end{aligned} \tag{189}$$

Express it by T_{ER}.

$$LD(T_{ER}) = K\log\left(\frac{1-\sqrt{1-T_p}}{1+\sqrt{1-T_p}}\cdot\frac{1+\sqrt{1-T_pT_{ER}}}{1-\sqrt{1-T_pT_{ER}}}\right) \tag{190}$$

Substitute Eq. (190) to Eq. (188), then we get the final formula of the distance modulus of LD to $z = 0.05$ as follows.

$$\begin{aligned} DM_{0.05}(T_{ER}) &= 5\cdot\mathrm{lg}\left(\log\left(\frac{1-\sqrt{1-T_p}}{1+\sqrt{1-T_p}}\cdot\frac{1+\sqrt{1-T_pT_{ER}}}{1-\sqrt{1-T_pT_{ER}}}\right)\right) \\ &-5\cdot\mathrm{lg}\left(\log\left(\frac{1-\sqrt{1-T_p}}{1+\sqrt{1-T_p}}\cdot\frac{1+\sqrt{1-T_p/1.05}}{1-\sqrt{1-T_p/1.05}}\right)\right) \end{aligned} \tag{191}$$

Fig. 28(a) is the graph of the distance modulus of Eq. (191), which is LD on a logarithmic scale, versus the redshift on a logarithmic scale (double-logarithmic graph). The dotted line is for the virtual case that the light speed is constant without change, and the solid lines are actual graphs where the light speed changes as the space expands. The blue line is for the case that the current cosmic radius is 0.8 times the maximum ($T_P = 0.8$), the red one is for 0.7 times, and the green one is for 0.6 times.

Fig.28. Magnitude of light propagated distance to $z = 0.05$

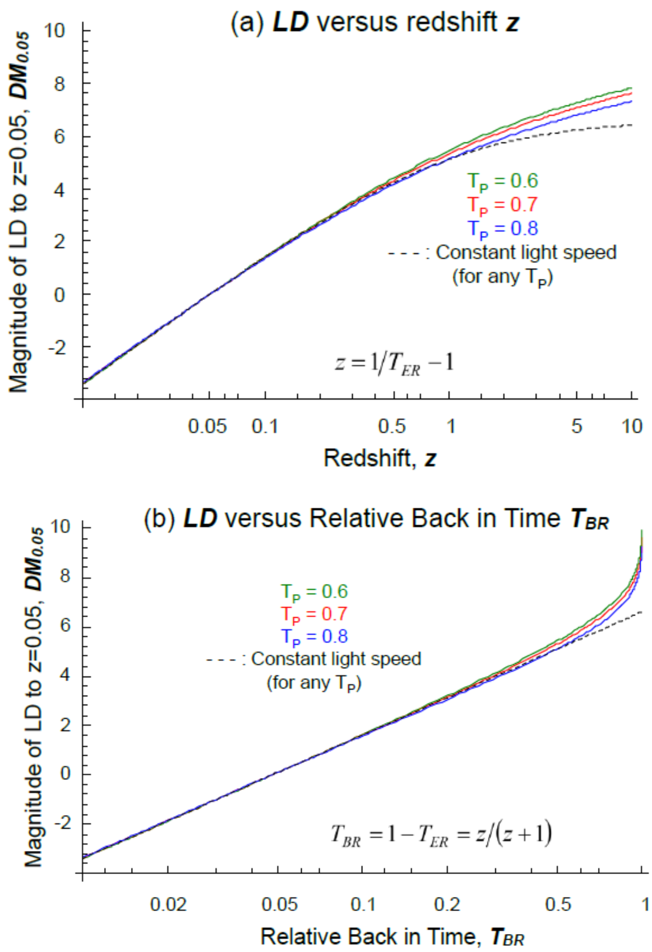

In Fig. 28(b), the horizontal axis T_{BR} is the time from the emission to the present instead of the redshift, given as below.

$$T_{BR} \equiv 1 - T_{ER} = z/(z+1) \tag{192}$$

The dotted line for the invariant light speed becomes a straight line, but in reality, due to the decrease in the light speed by the space expansion, distant stars show greater distances than a straight line. The Hubble's law states that the speed, with which a star moves away from us, is proportional to its distance, but this speed is not proportional to its redshift. The redshift should not be plotted on the horizontal axis to represent the Hubble's law, however, the most of reports have used the redshift on the axis in the Hubble diagram.

8.5. Data processing for Hubble diagram

The Hubble diagram is basically the graph of the present distance PD versus the redshift z. In the current astronomy, the brightness is converted to the present distance PD as a distance index, and shown in the Hubble diagram. The SCP (Supernova Cosmology Project) uses the following standard data processing, and obtains the values of PD as a distance index.

✧ **Time dilation**

The present distance is obtained by multiplying the distance LD, which is calculated from the brightness of a supernova, by the space expansion rate $n = z + 1$. (LD is called as the luminosity distance, but synonymous with the light propagated distance.) This conversion is called as the **time dilation**, but is actually incorrect. The measured distance is not the distance at the emission D_0, but is the light propagated distance LD. Therefore, it is necessary to use the conversion formula of Eq. (183).

The time dilation has another aspect. The horizontal axis in Fig. 28(b) is the value from the Time of emission to the present as T_{BR}, which is equal to $z/(z + 1)$. If we multiply both the vertical and horizontal axes by $(z + 1)$, the linearity of the line for the case of constant light speed is preserved. In this case, the horizontal axis becomes the redshift z. If we want to see the linearity with the redshift, we should perform only the time dilation multiplying LD by $(z + 1)$ without the K correction.

✧ K correction

Actually, in addition to the time dilation, a process called the **K correction** is performed. This converts a measurement at a redshift z to a measurement in the rest frame $(z = 0)$. It includes the cross-filter adjustment of the absolute magnitude depending on the wavelength used and the adjustment of the difference in the distance index among the two frames. The adjustment of the absolute magnitude is marginal, and the frame transformation of distance occupies most of the correction. We demonstrated that the frame transformation part of the K correction is equal to the conversion from LD to PD. Let us see details below.

Consider virtually a non-expanding universe, that is, a rest frame, by which the measured magnitude in the band X can be expressed as follows.

$$m_x^0 = M_x + DM^0 \tag{193}$$

M_x is the absolute magnitude measured in the band x and is the magnitude when the distance is 10pc (parsec). The reference target differs depending on a frequency band used, and there is sometimes a little difference in the absolute magnitude by bands. DM is the distance modulus versus the standard 10pc, and the above formula shows the change in brightness with distances. Since these elements are logarithmic, a sum shows a product of elements displayed on the normal scale.

If this star shows a redshift z and a magnitude m_y by the band y in the actual observation in the expanding universe, the difference from the above value in the rest frame is defined as the K correction.

$$K_{xy} \equiv m_y - m_x^0 \tag{194}$$

There is the following relation.

$$m_y = M_x + DM^0 + K_{xy} \tag{195}$$

On the other hand, in the actual observation showing the redshift z, m_y is given by the following formula.

$$m_y = M_y + DM(z) \tag{196}$$

Therefore, the K correction is shown as follows.

$$K_{xy} = M_y - M_x + DM(z) - DM^0 \tag{197}$$

The distance part of the K correction is as below.

$$K_{xy}^D = DM(z) - DM^0 \tag{198}$$

The difference in the absolute magnitude by a band to use is zero or very small, which falls in an observational adjustment. The distance part of the K correction is exactly the difference between the light propagated distance LD and the present distance PD in the logarithmic display, and corresponds to the LD-PD conversion. The K correction is a negative value because it takes the conversion from PD to LD by definition.

Doing the K correction is synonymous with converting the measured light propagated distance LD to the present distance PD as shown below.

$$PD = \frac{2(z+1)}{z+2} LD = \frac{2}{1+T_{ER}} LD \tag{199}$$

8.6. Comparison with supernova data in Hubble diagram

✧ Observed supernova data

In general, we cannot know the distance only from the brightness. Usually, once the redshift is measured, the distance is decided, and the luminosity is revealed from the Hubble diagram. In the case of Type 1a supernovae, the maximum luminosity is the same. Therefore, only from the brightness data, its distance can be obtained. Perlmutter, *et al*. reported their interim report in 1997, and the first full paper in 1999 from 42 type 1a supernovae. Then they concluded that the space expansion is accelerating. Since then, their project Supernova Cosmology Project (SCP) has added more data and obtained a quite precise Hubble diagram.

✧ Adjusted present time

In order to compare the Hubble diagram from the ECT with the reported one from the SCP, we take the same data processing as theirs. We add the **time dilation** and the **LD-PD conversion** corresponding to the K correction to the distance modulus of Eq. (191) as follows.

$$(1+z)PD = (1+z)\frac{2(z+1)}{z+2}LD \tag{200}$$

Express it by T_{ER}.

$$\frac{1}{T_{ER}}PD = \frac{1}{T_{ER}}\cdot\frac{2}{1+T_{ER}}LD \tag{201}$$

We named the left side as the adjusted PD. We get the "**adjusted magnitude of PD to z=0.05**" as follows.

$$\begin{aligned} DM_{0.05}^{adj}(T_{ER}) &= 5\begin{pmatrix}\lg LD(T_{ER}) + \lg(1/T_{ER}) + \lg(2/(1+T_{ER})) - \lg LD(1/1.05) \\ -\lg 1.05 - \lg(2*1.05/2.05)\end{pmatrix} \\ &= 5\begin{pmatrix}\lg LD(T_{ER}) - \lg(T_{ER}) - \lg(1+T_{ER}) - \lg LD(1/1.05) \\ -2\cdot\lg 1.05 + \lg 2.05\end{pmatrix} \end{aligned} \tag{202}$$

Substitute LD of Eq. (190), it becomes as follows.

$$\begin{aligned} DM_{0.05}^{adj}(T_{ER}) = 5\cdot\lg\left(\log\left(\frac{1-\sqrt{1-T_p}}{1+\sqrt{1-T_p}}\cdot\frac{1+\sqrt{1-T_pT_{ER}}}{1-\sqrt{1-T_pT_{ER}}}\right)\right) \\ -5\cdot\lg\left(\log\left(\frac{1-\sqrt{1-T_p}}{1+\sqrt{1-T_p}}\cdot\frac{1+\sqrt{1-T_p/1.05}}{1-\sqrt{1-T_p/1.05}}\right)\right) \\ -5\cdot\lg(T_{ER}) - 5\cdot\lg(1+T_{ER}) - 10\cdot\lg 1.05 + 5\cdot\lg 2.05 \end{aligned} \tag{203}$$

Its graph versus the redshift is given in Fig. 29. The redshift of the horizontal axis is on a logarithmic scale on the left and on a normal scale on the right. Even the dotted line for the virtual case of constant light speed is not a straight line on the left.

Fig. 29. Adjusted magnitude of Present Distance to $z = 0.05$

The adjusted magnitude of PD to $z = 0.05$, $DM_{0.05}^{adj}$ versus the redshift $z = 1/T_{ER} - 1$

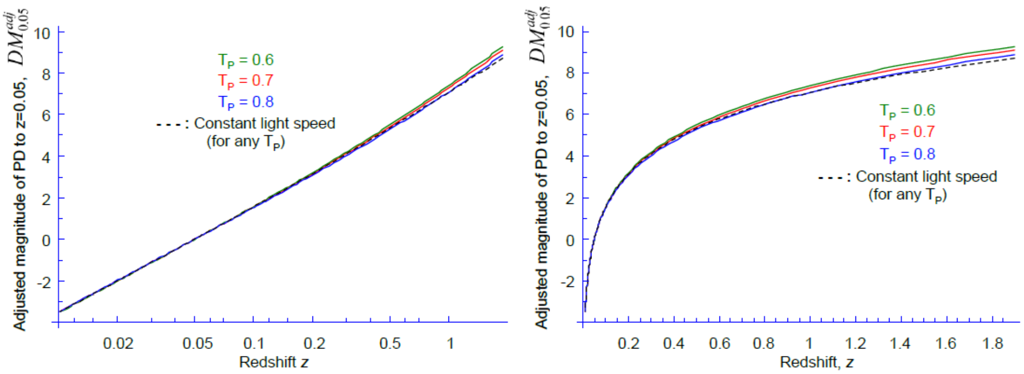

- - - - : reference $DM_{0.05}^{adj}$ based on $LD_C = c \cdot T_P(1 - T_{ER})$ subject to constant light speed

✧ Overlay of the adjusted magnitude of PD with supernova data

Finally, let us compare the above Hubble diagram from the ECT with the observed data of Type 1a supernovae. Fig. 30 is an overlay of the graphs of Eq. (203) for the adjusted present time and the observed values of supernovae from the SCP, which Rubin, *et al*. reported in 2013.

As we see in Fig. 30, there is an excellent fit to the observed supernova data. The scale of the vertical axis is different among the two graphs because the reference distance is different. In actual measurements, the distance values at the same redshift vary. This is due to the Doppler effect based on the movement of individual stars.

Although it is not shown in Fig. 30, the graph for the virtual case that the light speed has been constant is below the curve for the present time (radius) is $T_p = 0.8$. As we see there, $T_p = 0.7$ showed an extremely good agreement with the observed data, and its line is very closely overlapping the line of flat $\Omega_m = 0.27\Lambda\mathrm{CDM}$ universe that Rubin *et al* concluded as the best fit. ($\Omega_m = 0.27\Lambda\mathrm{CDM}$ is the model consisting of 73% dark energy, cold dark matter, and observable matter.)

Fig. 30. Overlay of Hubble diagram from ECT and SCP data

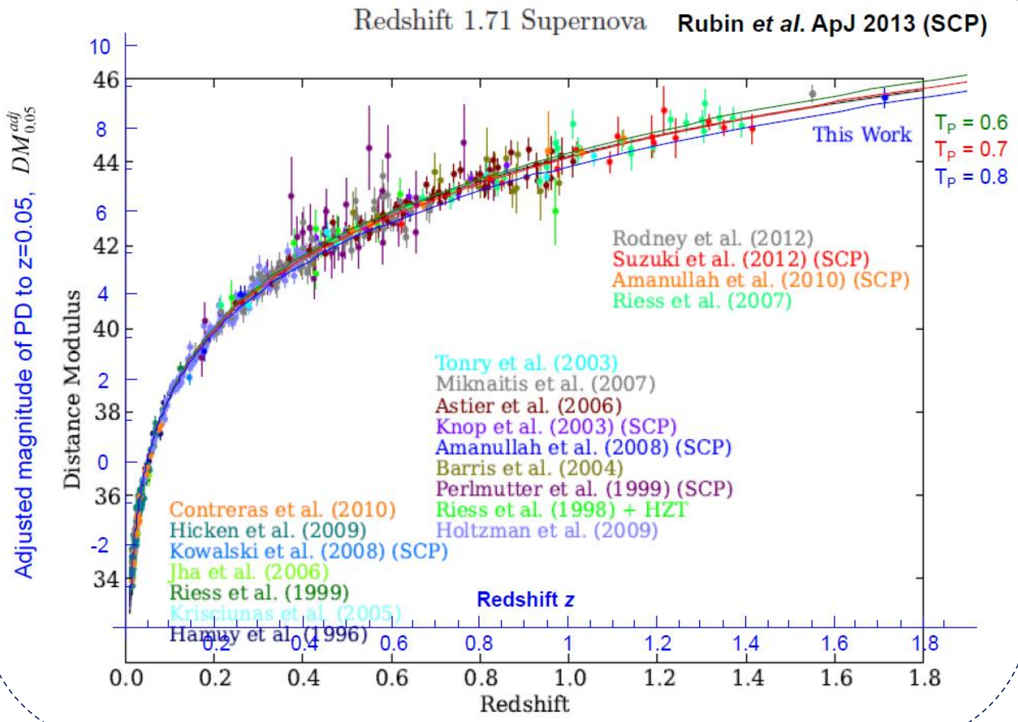

As we saw in this chapter, we can conclude that the observed supernova data imply the variation of the light speed by the space expansion but never the acceleration of the expansion speed. Dark energy that is expected to accelerate the space expansion by the standard physic does not exist. Provided, the vacuum space of the universe is filled with the space energy.

Chapter 9: Overall picture of cosmic evolution

9.1. Stages of cosmic evolution

We have seen the evolution of the universe in this book. Let us divide the cosmic evolution into main stages.

(0) Cosmic separation

This is the initiation of the universe, which corresponds to the inflation and big bang in the standard cosmology. By the cosmic separation, two universes were generated. It is an open question whether the two universes will continue to recede or whether they will turn to move closer. From only the fundamental force, they would continue to recede. However, we assume that they would turn to get closer by the gravitational force in the long future.

(1) Stage of cyclic decompositions of early energy circulations

This is the stage explained in the Section 5.1. By many rounds of cyclic decompositions, countless galactic seeds were born as well as the large-scale structures of the universe. In this stage, lots of energy radiations were emitted, which we will explain in the Section 9.2.

(2) Stage of galactic seed separations

This is the stage explained in the Section 5.2. As explained in the Sections 5.3 and 5.4, gamma-ray bursts happened due to the decrease in potential energy. Resulting galactic seeds are in three types as a source of galaxy; isolated, rotating binary, and attached two galactic seeds.

(3) Stage of stellar seed releases

After completion of galactic seed separation, each galactic seed started to release stellar seeds and formed a galaxy.

For individual galaxies, those three stages are in series without overlapping. However, as the whole universe, the three stages include large overlaps. The Stage (2) is characterized by gamma-ray bursts. Among the reported GRBs, the most distant one is 13.1 billion light years ($z = 9.4$), and the least distant one is 0.13 billion light years ($z = 0.0097$). We can guess that the event of any galactic seed separations started more than 13.1 billion years ago and terminated around 130 million years ago.

9.2. Cosmic microwave background CMB

As the final piece of cosmic evolution, let me explain the **cosmic microwave background CMB**.

The CMB is observed almost isotropically from all directions in the universe. It has a frequency distribution almost same as that of a black body radiation at an absolute temperature of 2.7 K. In the standard cosmology, this is regarded as the evidence of the Big Bang theory that the universe started from an extremely high temperature and density state, then has become a low temperature and density state due to the space expansion. The standard cosmology claims that only high energies existed at first, then matter-antimatter pairs were generated from them. However, the model is incorrect as we have explained in this book.

A cyclic decomposition of an early energy circulation in the Stage (1) is an event of simultaneous orthogonal separations, and releases a lot of extremely high energies due to the decrease in potential energy. The released energies were primarily radiations, then excited spacias and generated elementary circulations such as iS, iD, S, D, and their excited forms.

As explained in the Section 7.3 for energy of eCPs by the equations from Eq. (132) to Eq. (138), the releases and absorptions of light among many eCPs by shortening or prolonging their lengths occurred randomly. After repeating such a light release and absorption, the radiated lights reached an equilibrium state consisting of many harmonic wave components. This is similar to the thermal equilibrium.

High-energy light causes a division of an eCP to two ones. In the case of an eCP in an atom, it divides to a proton and a free electron, which are in the plasma state. In the plasma state of the early-stage universe, the light could not propagate straight, but was scattered by absorption and emission. After the space expanded to a certain level, the space got transparent to light, we call the timing of which as the "**Time clear**" T_c. After T_c, most of the lights of that time came to us without changing. The set of wavelengths has been expanded by the space expansion (redshift), and is now observed as a microwave distribution similar to that of the thermal equilibrium at 2.7 K. This is the feature of the CMB.

Closing

Thank you for reading to the end of this book. It should be too long to read, but I tried to explain the cosmology by the ECT precisely and logically as much as possible. This book covers the four original papers of [1],[3],[5], and [6], as one reading to develop the cosmic evolution.

As you see in this book, the ECT has successfully revealed almost all the processes of the cosmic evolution; from the birth of the universe to the present figures, starting from the definition of energy and the two premises. It is a big contrast to the existing cosmology by the standard physics, in which too many very important matters are left as unknown or not yet discovered. The chaotic situations of the standard physics should be because they did not know the force working based on momentums.

Not only the cosmology, the ECT has derived the novel particle physics [2], quantum mechanics [4], and electromagnetism [7]. Despite these overwhelming successes with the ECT, will you still stick to the existing standard physics, which are shelving important things as open questions?

May 2024

Shigeto Nagao

Posted in Books on the ECT

http://www3.plala.or.jp/MiTiempo/books.html